Calibration: Criticality and Creativity

by

Dr. G. Charmaine Gilbreath
U. S. Naval Research Laboratory
Washington DC 20375

Charmaine.gilbreath@nrl.navy.mil
202-767-0170

NRL Publication Release: 14-1231-2712; Distribution is Unlimited

Without CALIBRATION, we cannot trust our science or our engineering instruments.

It is the most important FIRST EXERCISE to undertake for every level of research and development.

• Layer One:	Sensor
• Layer Two:	Instrument
• Layer Three:	Subsystem
• Layer Four:	System
• Layer Five:	Reference Baseline for Phenomenology

Calibration is a comparison between measurements – one of known magnitude or correctness made or set with one device and another measurement made in as similar a way as possible with a second device. The device with the known or assigned correctness is called the standard.

The formal definition of calibration by the International Bureau of Weights and Measures is the following: "Operation that, under specified conditions, in a first step, establishes a relation between the quantity values with measurement uncertainties provided by measurement standards and corresponding indications with associated measurement uncertainties (of the calibrated instrument or secondary standard) and, in a second step, uses this information to establish a relation for obtaining a measurement result from an indication.“

In Analytic Chemistry:

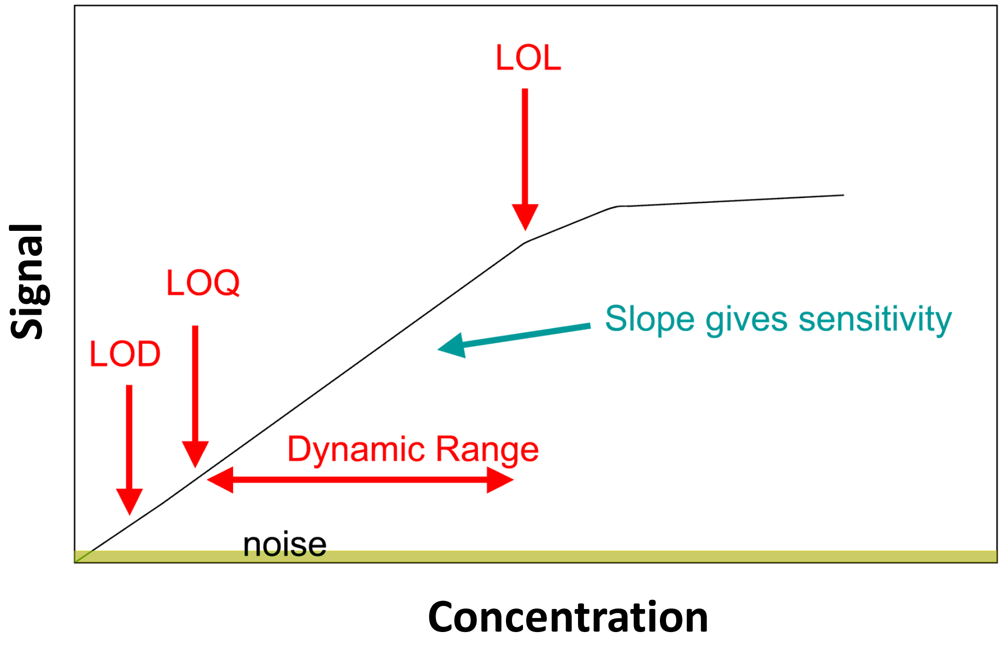

A calibration curve plot showing limit of detection (LOD), limit of quantification (LOQ), dynamic range, and limit of linearity (LOL).

$$s_x = \frac{s_y}{|m|}\sqrt{\frac{1}{n} + \frac{1}{k} + \frac{(y_{unk} - \bar{y})^2}{m^2 \sum (x_i - \bar{x})^2}}$$

Error in calibration curve results[edit]

s_y is the standard deviation in the residuals = $\sqrt{\frac{\sum (y_i - m x_i - b)^2}{n-2}}$

m is the slope of the line

b is the y-intercept of the line

n is the number standards

k is the number of replicate unknowns

y_{unk} is the measurement of the unknown

$\bar{y}$ is the average measurement of the standards

x_i are the concentrations of the standards

$\bar{x}$ is the average concentration of the standards

http://en.wikipedia.org/wiki/Calibration_curve

CALIBRATION in the context of Remote Sensing

Data flow for calibration of remote sensing images to physical units for surface reflectance (*)

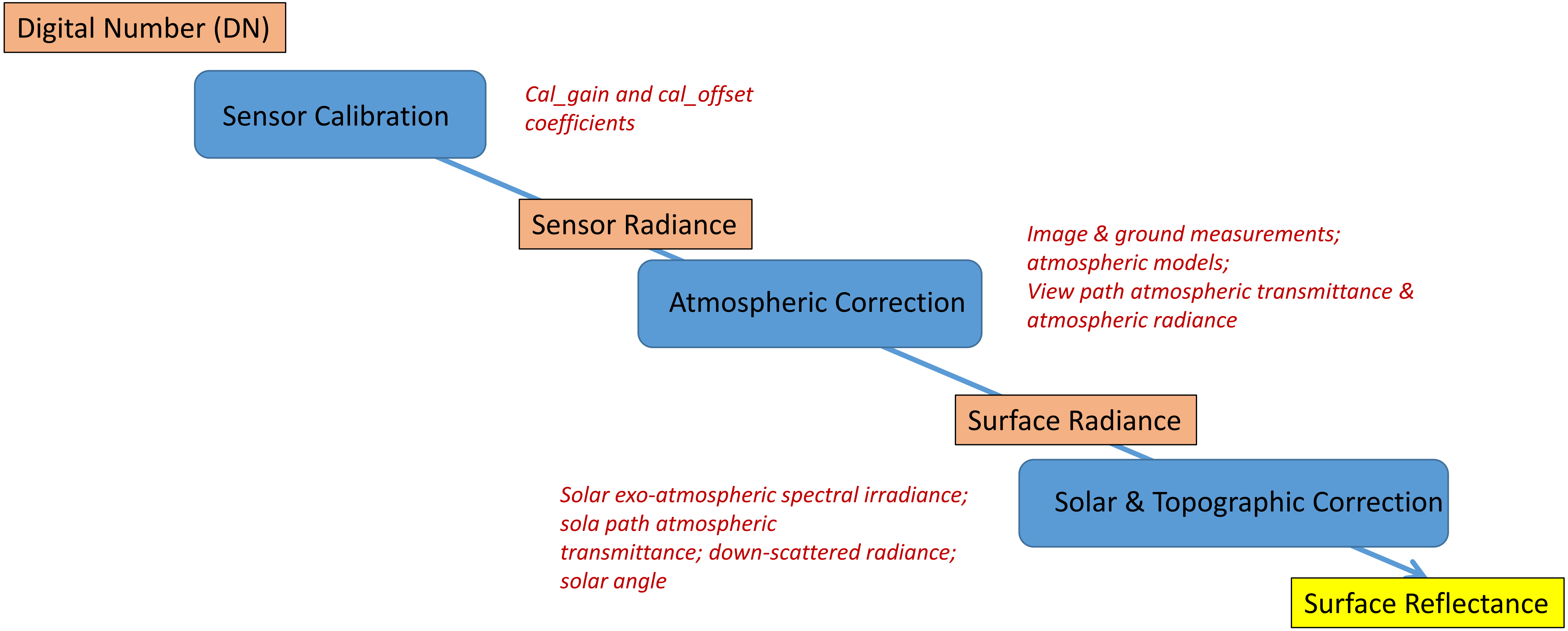

* Schowengerdt, Robert A., *Remote Sensing: Models and Methods for Imaging Processing*, Third Edition, Elsevier Publishing, (2007), pp. 333-335.

See: Typical Calibration Equations and Parameters for Imaging Radiometers:

Irradiance Calibration Equation (for point sources)

Radiance Calibration Equation (for extended sources)

In Draft: *Guidelines for Radiometric Calibration of Electro-optical Instruments for Remote Sensing,* Joseph Tansock, and 20 additional contributors, 2014

Navy/DoD Relevance of Ionosphere and Thermosphere Effects

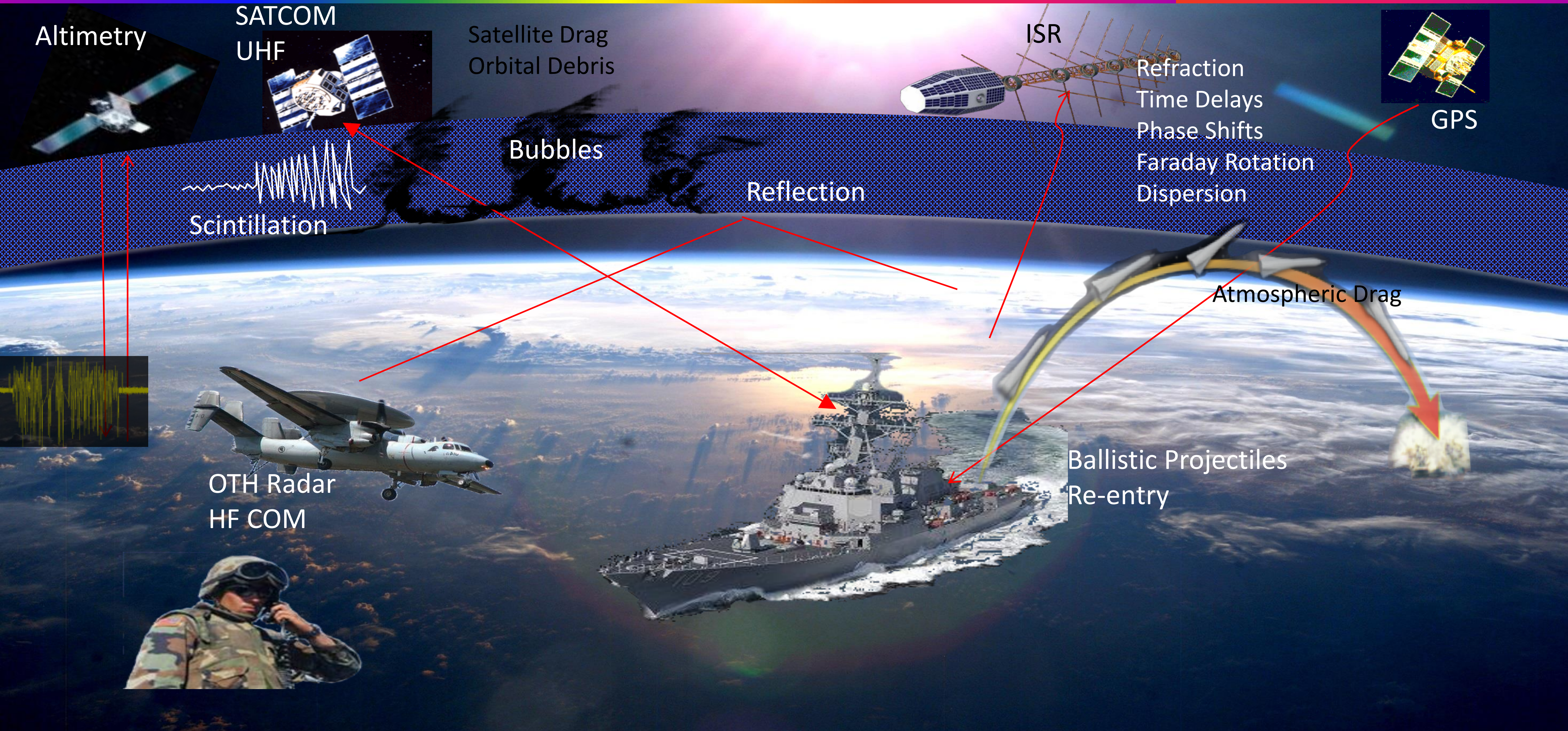

Material courtesy of SSULI: Distribution is Unlimited

Description

- Special Sensor Ultraviolet Limb Imager (SSULI)
  - Was proposed in response to a Joint Chiefs of Staff memo [MJCS 154-86] recognizing the need to characterize the presence and behavior of electrons and electrically neutral particles in the ionosphere
  - Is an operational optical remote sensor integrated on the operational Air Force Defense Meteorological Satellite Program (DMSP) spacecraft

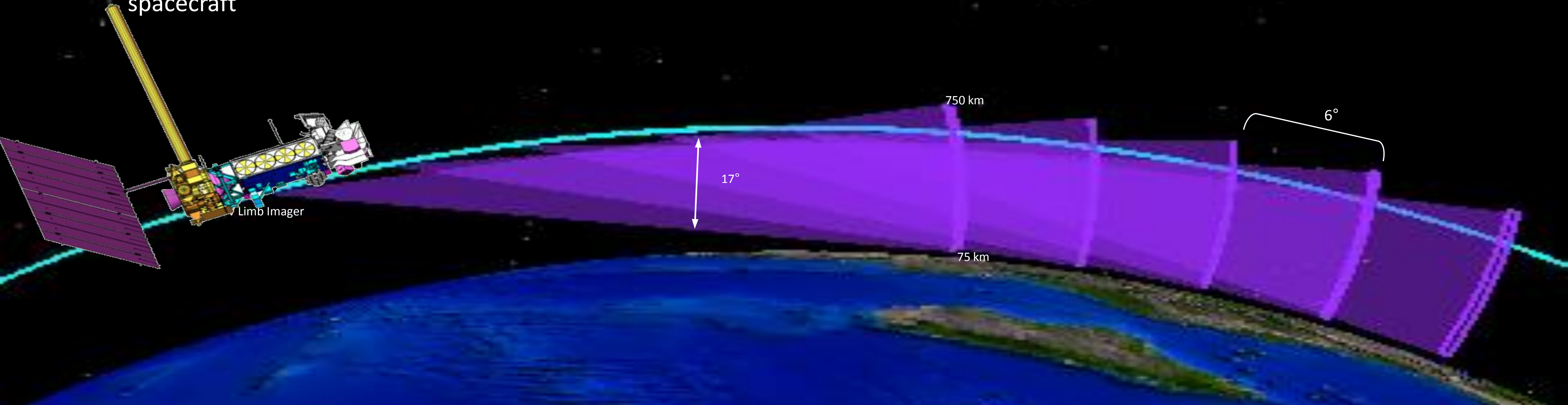

  - Views the Earth's limb at a tangent altitude of approximately 50 km to 750 km
  - Measures vertical profiles of the natural airglow radiation from atoms, molecules, and ions in the upper atmosphere and ionosphere
  - Measurements are made from the extreme ultraviolet (EUV) to the far ultraviolet (FUV) over the wavelength range 80 nm to 170 nm
  - Measurements used to determine the electron density and neutral density profiles of the emitting atmospheric species

Global Ionospheric Weather: Daily Post-Sunset Ionosphere for 2010 and 2011

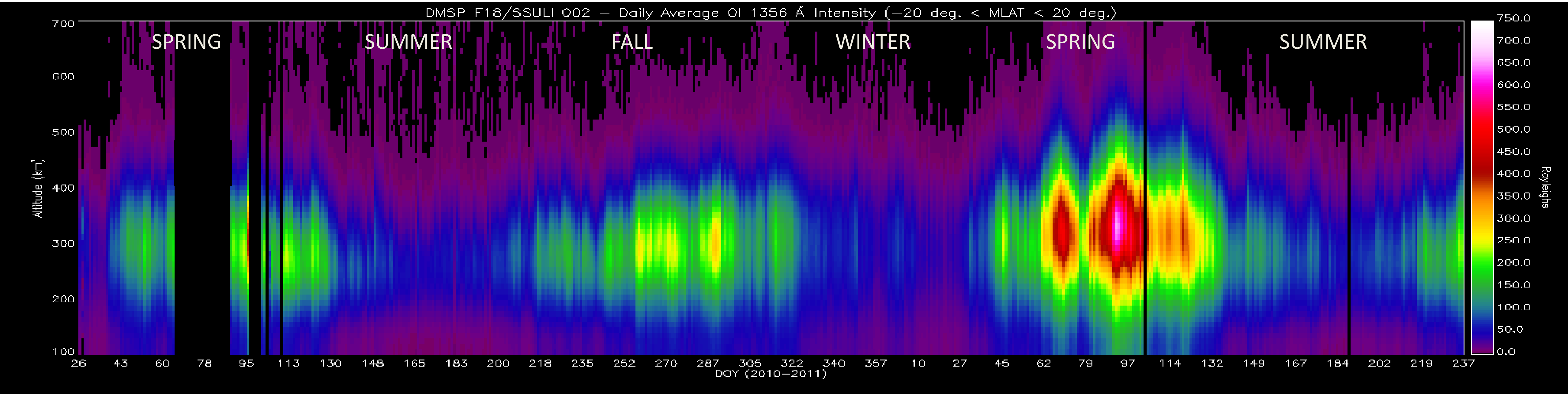

Daily average of SSULI Oxygen ion emission profiles (SDRs) – validated using ground truth.

SSULI captures the ionospheric weather – daily response of the low latitude ionosphere to atmospheric forcing from below (weather) and magnetospheric forcing from above (space weather).

Emission profiles (SDRs) ingested by GAIM assimilation model at AFWA - currently operational

Local time of DMSP F18 orbit (2030LT) observes largest ionospheric gradients - plays a critical role in ionospheric specification and scintillation forecasting.

Calibration Methodology – Preflight

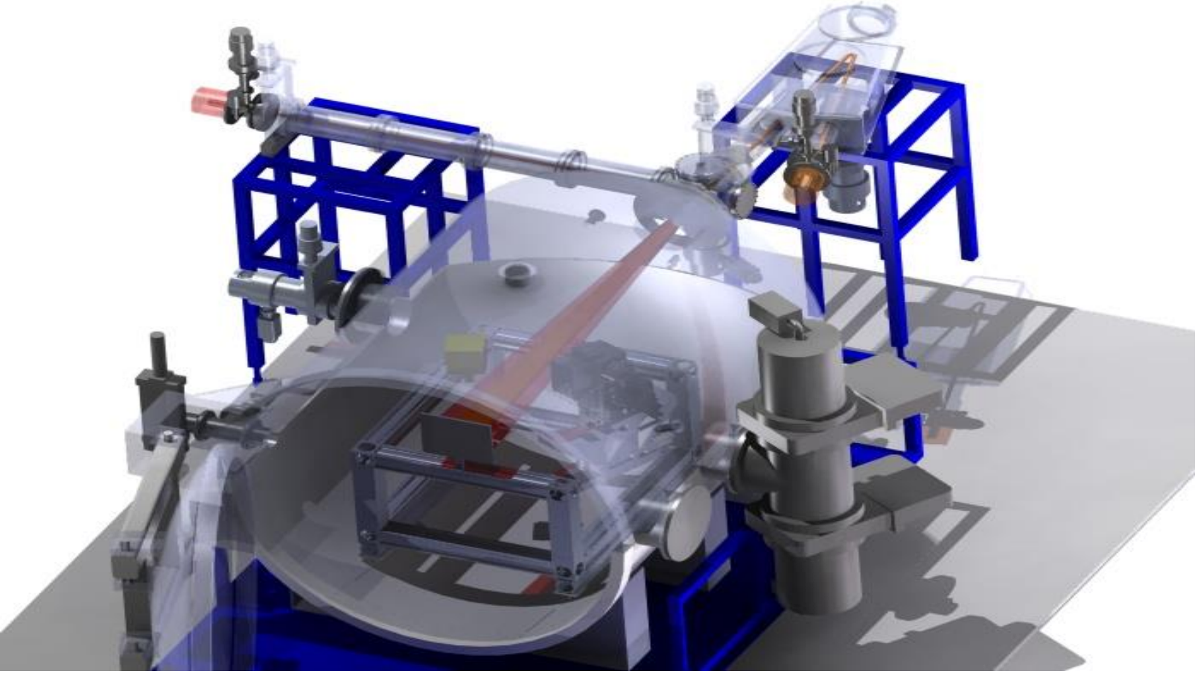

SSULI Calibration Chamber

- **Orange light path indicates monochromator illumination of diffuser**
- **Red light path indicates direct lamp illumination of diffuser**
- **SSULI (black) and reference detectors (gold) are inside chamber, staring at diffuser**

- SSULI sensitivity calibration provides three sets of instrument characteristics
  - Detector mapping (wavelength to pixel)
  - Sensitivity measurement
  - Resolution and line shape measurement
- Calibration takes place in two stages
  - Relative Calibration – does not fill SSULI FOV
    - Using a monochromator, 20+ individual emission features studied
    - create a calibration curve with an unknown offset
    - Line shapes are good, but underestimate the near wings
  - Absolute Calibration – fills SSULI FOV
    - 2 emission features are studied
    - Offset to relative cal. curve determined
  - All sensitivities are measured relative to a NIST-calibrated channeltron and g-tube photomultiplier

On-Orbit Stellar Spectra

- Aspect Solution
  - Effective pointing offset (0.20-0.35 deg)
  - Horizontal Field-of-view (2.5 deg FWHM)
  - Vertical Field-of-view (~0.17 deg FWHM)
  - Scan Mirror Accuracy (0.01 deg)
- On-orbit Calibration
  - Overall Sensitivity Monitoring
  - 2-D Detector Mapping
    - Characterized and diagnosed and F16 detector issue
    - Now monitors operational F18, F19 SSULI performance
  - Limited Gain Mapping (Possible)

On Orbit Horizontal FOV Results

- **Horizontal FOV**
  - **5 stars**
    - **HD 144217**
    - **HD 143275**
    - **HD 143018**
    - **HD 142669**
    - **HD 138690**
- **Scatter at peak**
  - **Sub-second dead time**
  - **Errors in automated background subtraction**
  - **Varying levels of noise**
- **Similar to lab profile**
  - **Field-filling differences**
- **FWHM 2.4º**

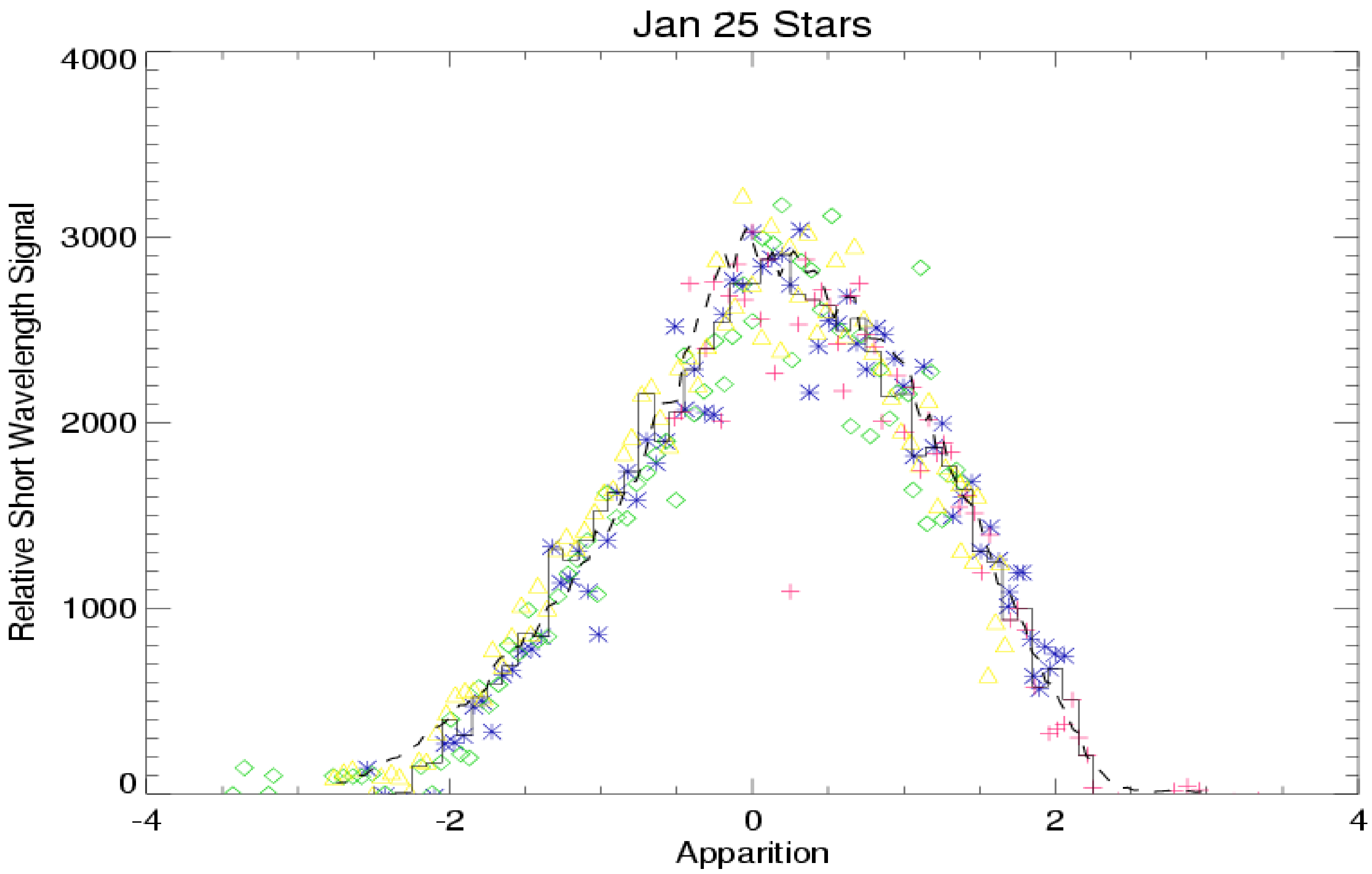

Contact: Scott Allen Buzdien, Ph.D., Geospace Science and Technology Branch; Code 7634, Naval Research Laboratory, 4555 Overlook Ave SW, Washington, DC 20375; 202-767-9372 scott.budzien@nrl.navy.mil

Thermospheric Density Fluctuations Derived from the Atmospheric Neutral Density Experiment Missions

A.C. Nicholas, M. Davis, T. Finne, S.A. Budzien, J. DeYoung, L. Healy, R. Kessel

Naval Research Laboratory

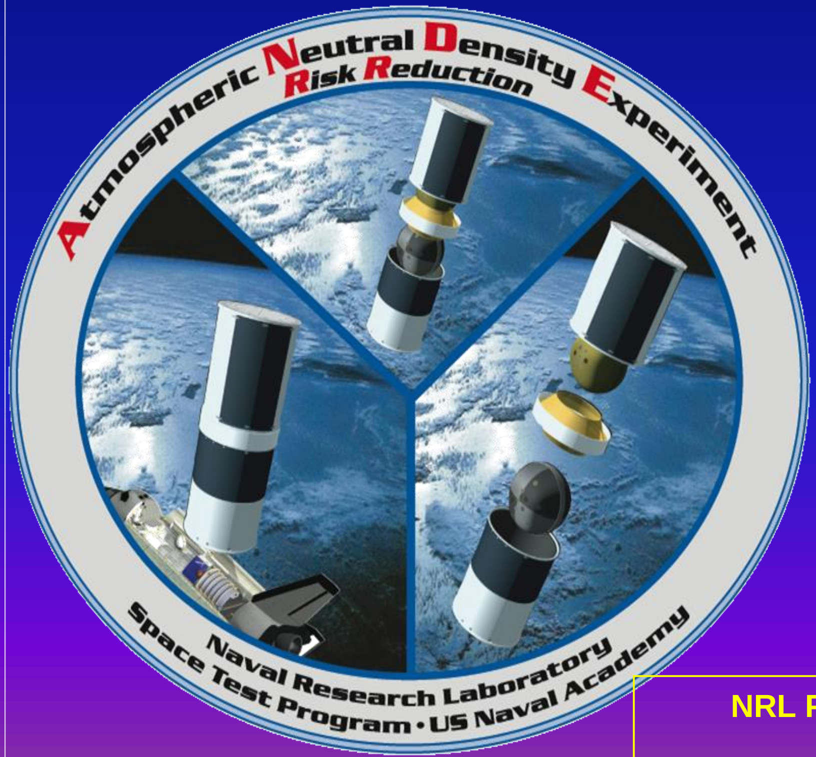

NRL Publication Release: 10-1226 1798
Distribution is unlimited.

ANDE Concept

Objectives:

1. **Provide Total Atmospheric Density for Orbit Determination and Collision Avoidance**
2. **Validate Fundamental Theories on the Calculation of the Drag Coefficient**
3. **Provide Calibration Objects for SSN**
4. **Establish a Method to Validate Neutral/Ion Density & Composition Derived from DMSP Sensors.**

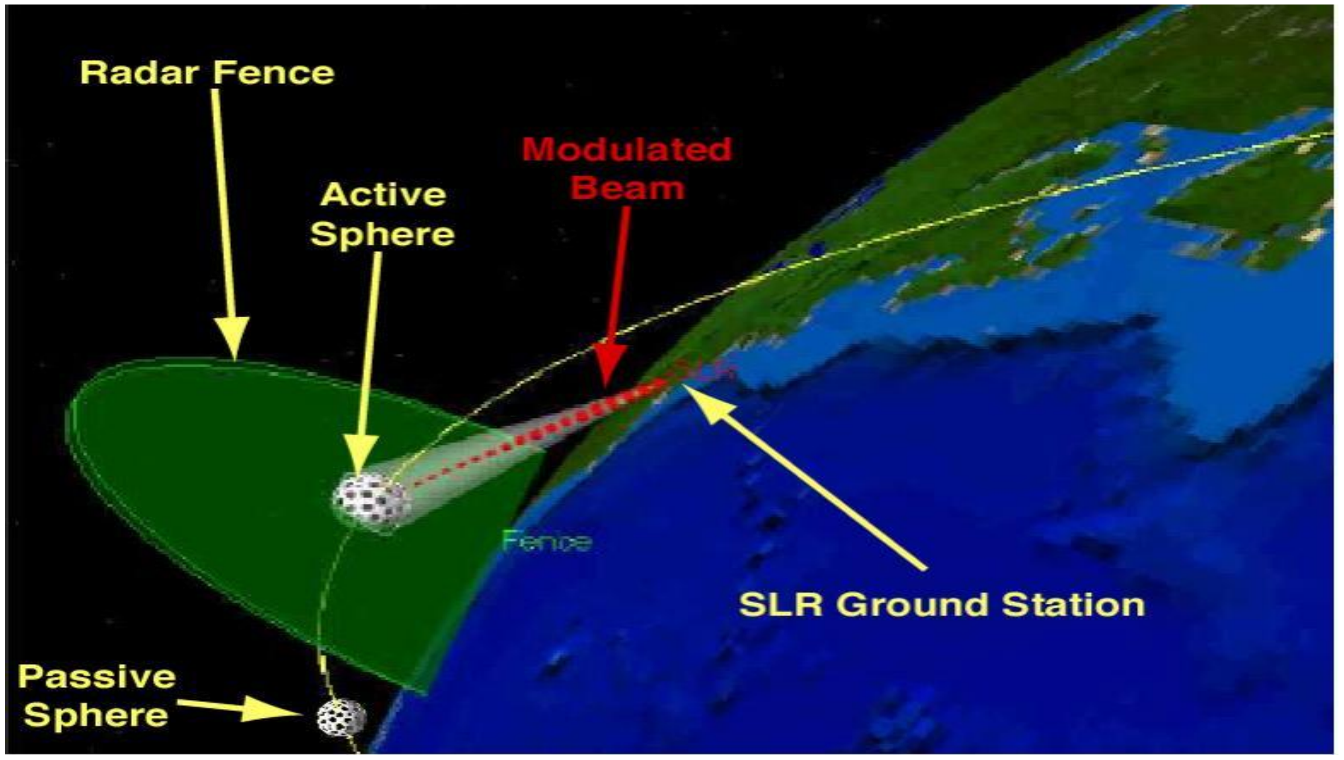

•Description:

•Fly two 19" spheres in lead-trail orbit
- **•400 km orbit**
- **•51 Degree inclination**

•Passive Sphere (~25 kg)
- **•Observed with SSN and SLR; variation in observed position used to determine in-track total density**

•Active Sphere (~50kg)
- **•Determine position wrt to passive sphere**
  - **•Compute total density**
  - **•Validate C_D models**
- **•Use on-board instrumentation to calculate density and composition**
- **•Launch via Shuttle in CY 2009**
- **•RR deployed 21 Dec 2006**

•Point of Contact

Andrew Nicholas

202-767-2441

andrew.nicholas@nrl.navy.mil

Mass Properties

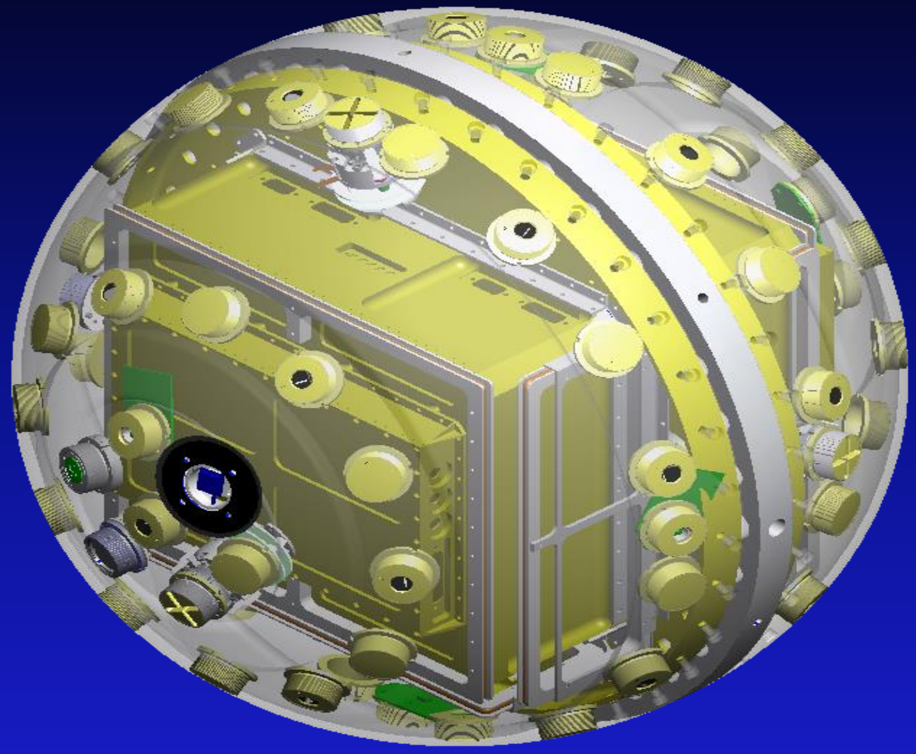

Castor

Diameter	19” Sphere
Mass	47.45 kg
Ixx (kg-m^2)	1.1645
Iyy (kg-m^2)	1.0753
Izz (kg-m^2)	1.0750

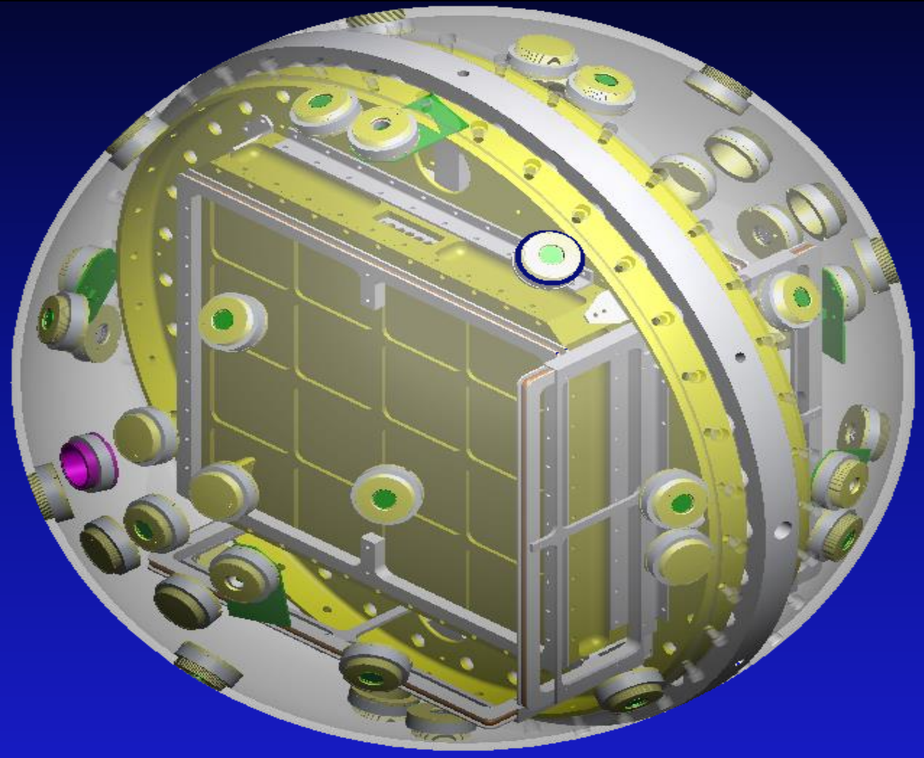

Pollux

Diameter	19” Sphere
Mass	27.44 kg
Ixx (kg-m^2)	0.8323
Iyy (kg-m^2)	0.6709
Izz (kg-m^2)	0.6702

Drag Equation

$$A_{Drag} = -1/2\rho BV^2$$

- Atmospheric density (ρ) is #1 source of error in LEO OD process
  - Current atmospheric density models are empirical climatological models (MSIS, Jacchia, all with 15% to 25% error inherent).
  - Sparse direct measurements of atmospheric density for validation.
- $B = C_D A/m$, inverse ballistic coefficient (B)
- Coef. of drag (C_D), modeled
  - Function of size, shape, material, roughness, temperature, atmosphere…
- Frontal Area (A) of spacecraft
  - Spherical symmetry is independent of orientation
- Mass (m) of spacecraft
- Velocity wrt medium $V=v_{sc}-v_m$
  - Winds; 5-10% of v_{sc} during geomagnetic storms
- Observe V, solve for product of ρB
  - Minimize variations in B to maximize accuracy of ρ

C_D Results

- Orbit determination derived C_D values (MSIS residuals) are non-physical!
  - These are results from 3-day fit spans; fitting product of ρB
  - Atmospheric models are over estimating density (ρ) ∴ resulting in an artificially low C_D
  - Consistent with secular change work of Emmert et al. (GRL, 2008)

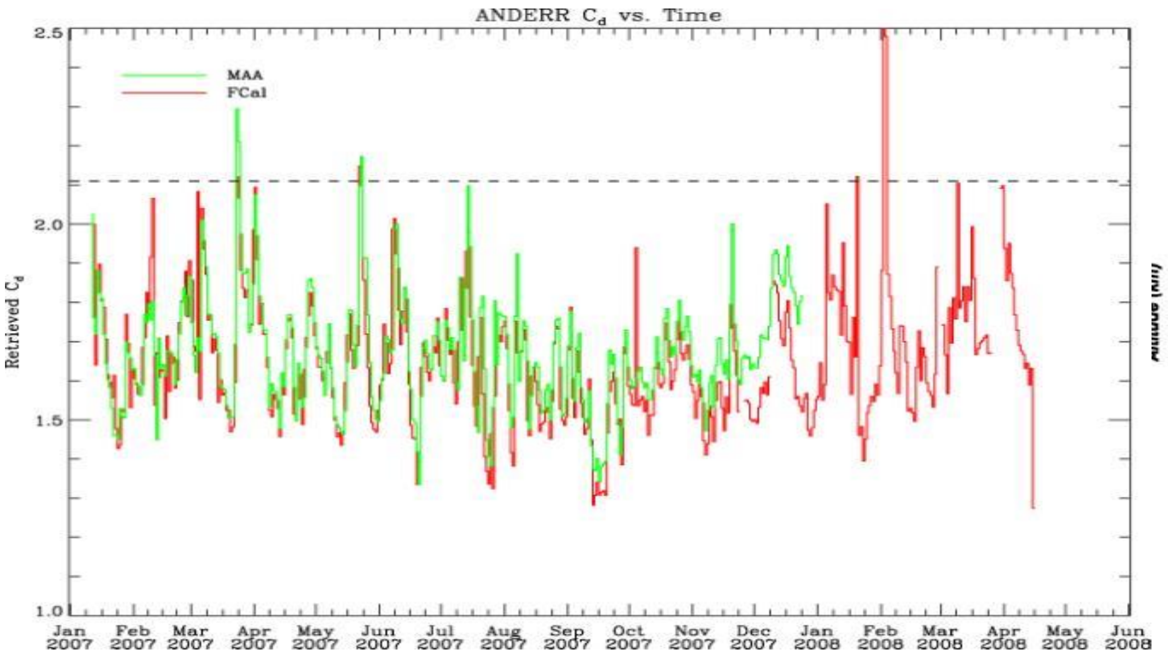

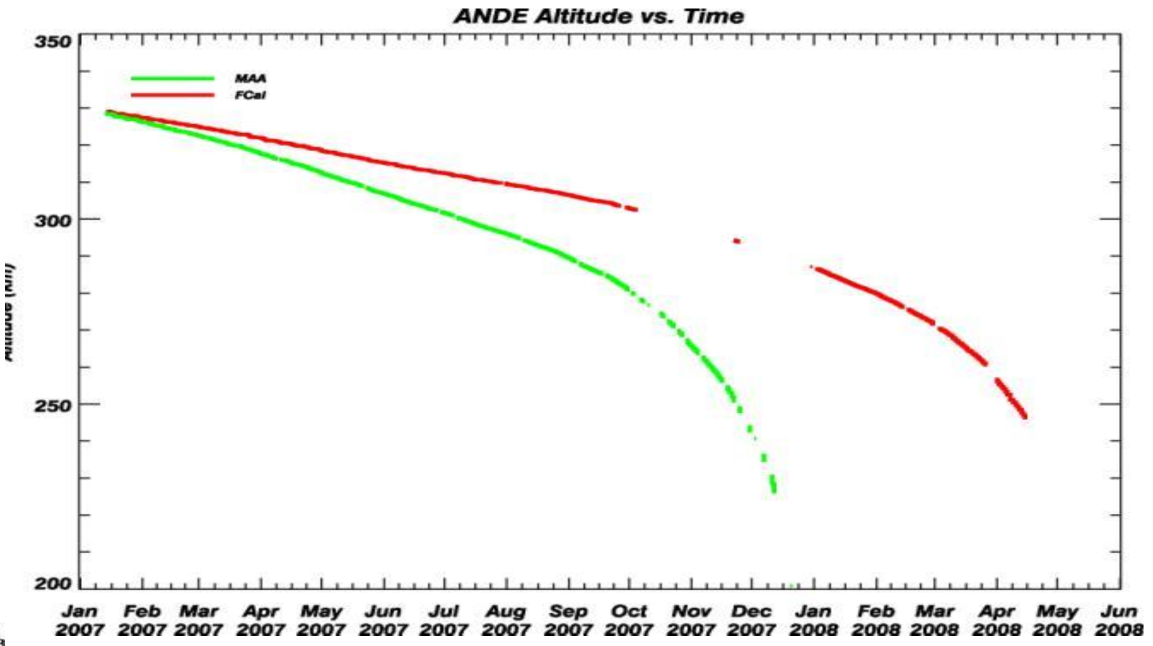

Object	Avg. Fitted C_D	Std. Dev.	MSIS Scale
MAA	1.67	0.156	0.790
FCal	1.65	0.168	0.783

Summary

It is clear that the ANDE2 spacecraft are useful calibration targets due to their well-characterized size and shape.

Atmospheric Models:

1. ANDE2 data show that both the MSIS and the Jacchia 70 atmospheric models are over estimating the total atmospheric density by ~25% or more, which is consistent with the findings of Emmert and Picone (JGR, 2008). The ANDE mission data will play a critical role in updating these models.
    - Currently an unfunded effort.
2. Runs from both models show correlation of the retrieved B with atmospheric drivers (solar and geomagnetic)
3. In 2007 both models results had about the same bias, in 2009 the J70 model is correcting for the bias in 2009 better than the MSIS model, perhaps due to a balance of low Ap and low F10.7 drivers.
4. MSIS results show considerably less scatter than Jacchia 70.

Contact: Andrew Nicholas, Ph.D., Space Science Division, Code 7634, Naval Research Lab., 4555 Overlook Ave SW, Washington, DC 20375; 202-767-2441; andrew.nicholas@nrl.navy.mil

Depth Perception in Augmented Reality

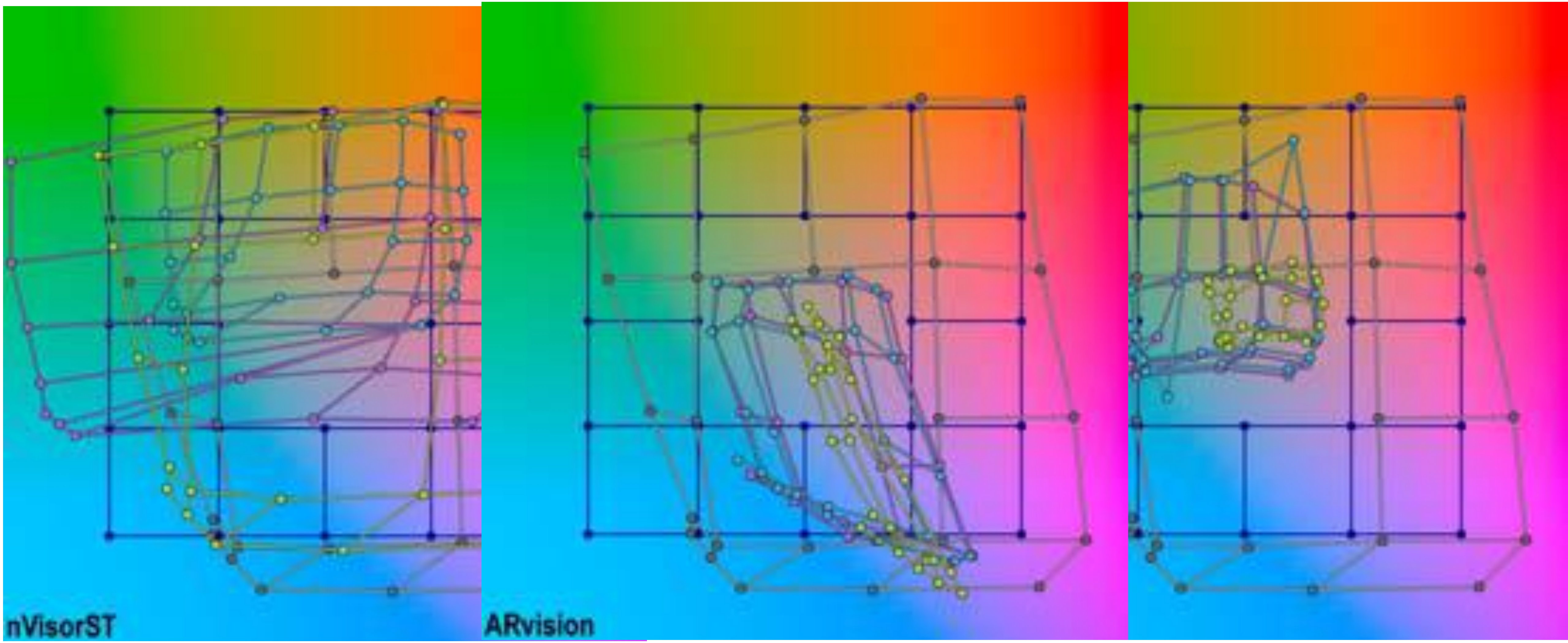

NRL Publication Releases: 12-1231-0309 and 12-1231-0310; Distribution Unlimited

Depth Perception in Augmented Reality

The Military Problem

When engaged in military operations in urban terrain, one challenge is maintaining situation awareness of troop locations. The augmented reality (AR) metaphor of “X-ray vision” can overcome this limitation, but graphics must be designed to intuitively convey relative depth among occluding real and virtual objects.

Experimental Evaluation of Depth Perception

We (NRL, Livingston, et.al.) have been conducting experiments to measure the depth perception conveyed by AR displays. Subjects were able to match the depth of real and virtual objects, with limiting factors being the presence of an occluding object in the area where the virtual object was depicted and the distance of the real object. Subjects had similar performance with a real-to-real depth matching task. Tests outdoors yielded some results that conflict with indoor tests.

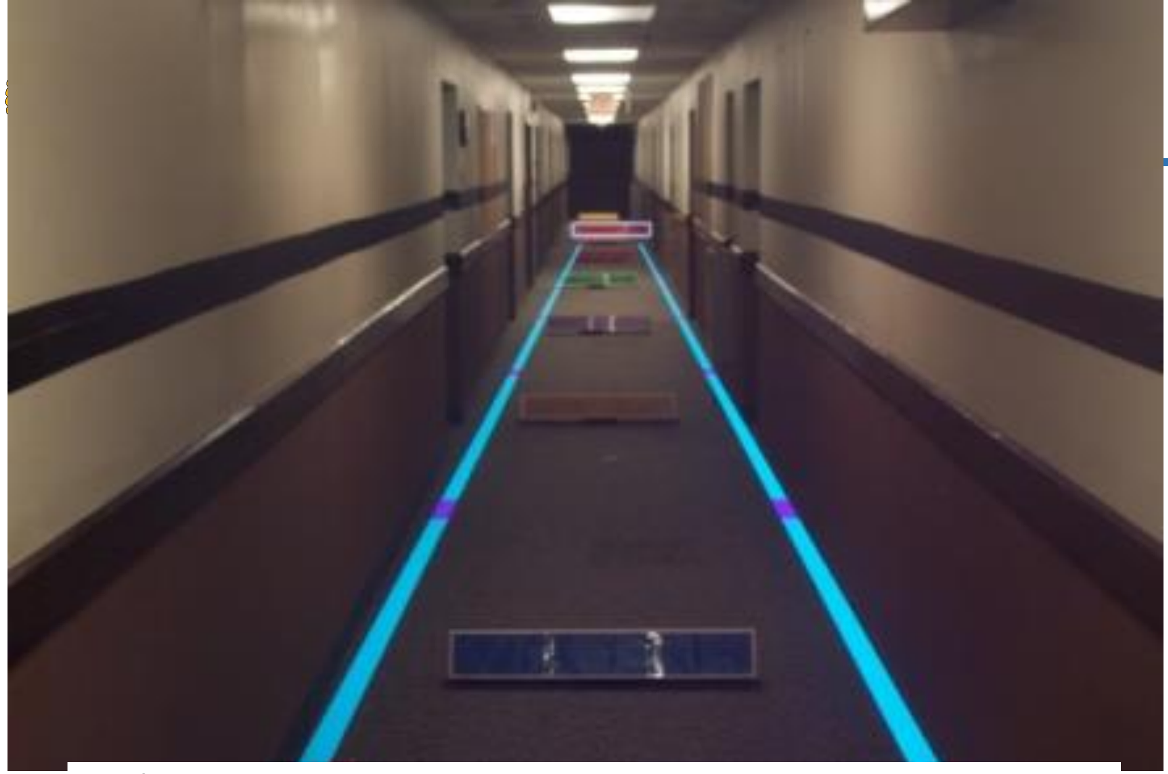

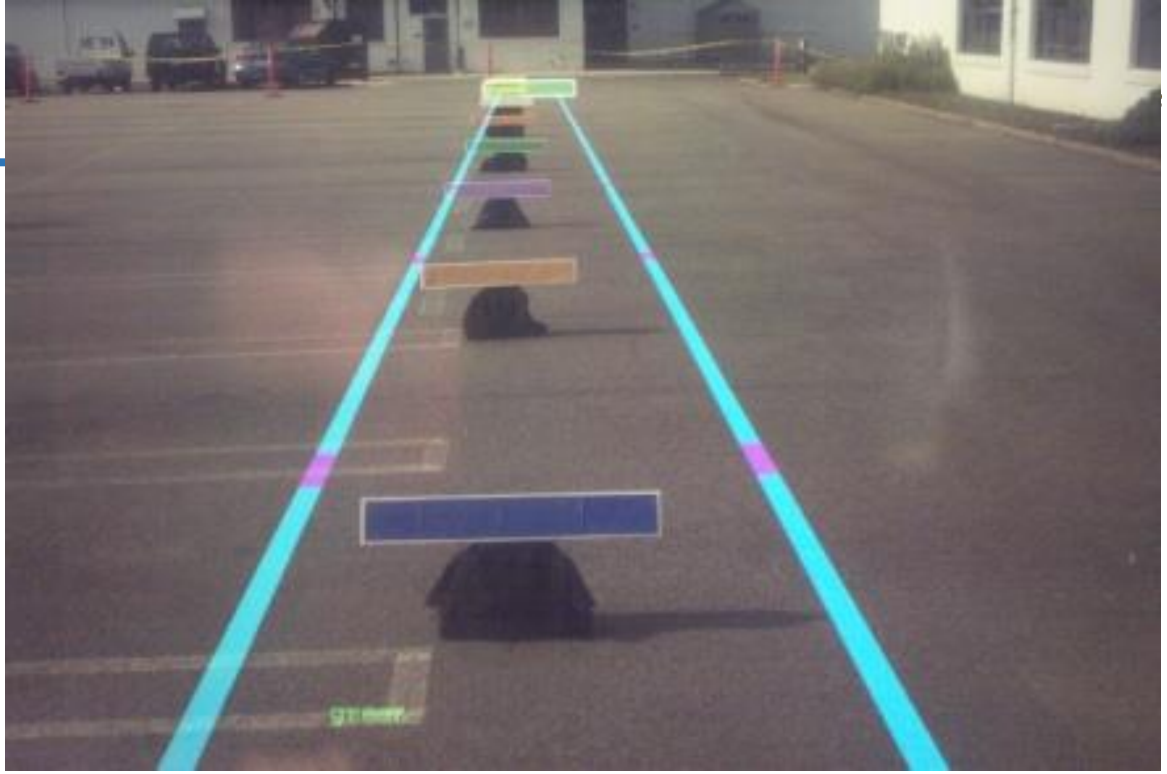

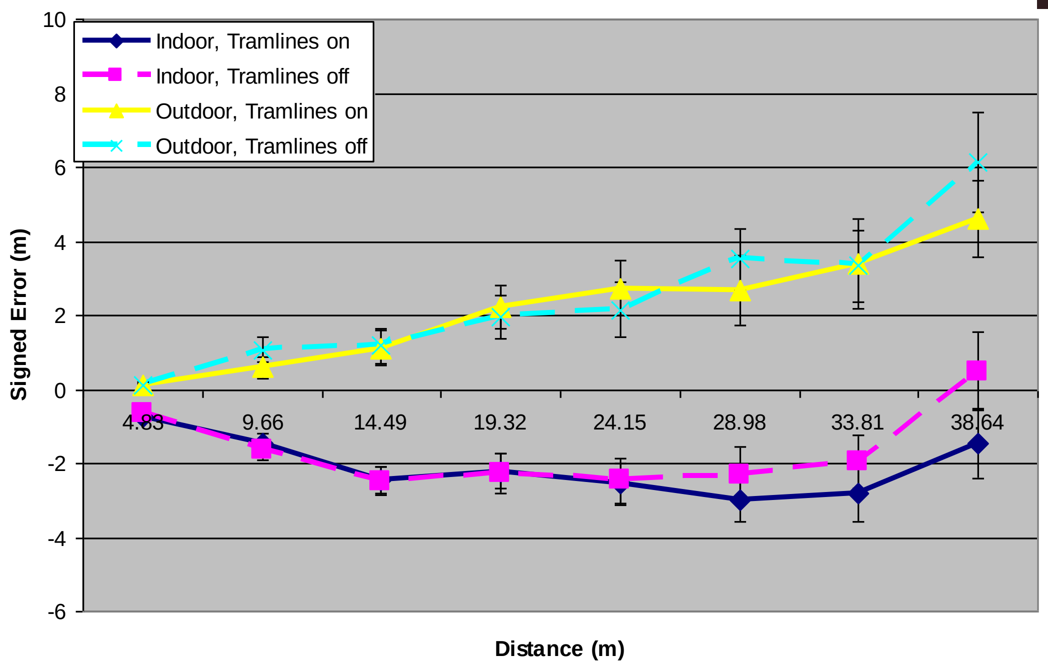

Contact: Mark A. Livingston, Ph.D., Virtual Environments and Visualization, Code 5581, Naval Research Laboratory, 4555 Overlook Ave SW, Washington, DC 20375; 202-767-0380 mark.livingston@nrl.navy.mil

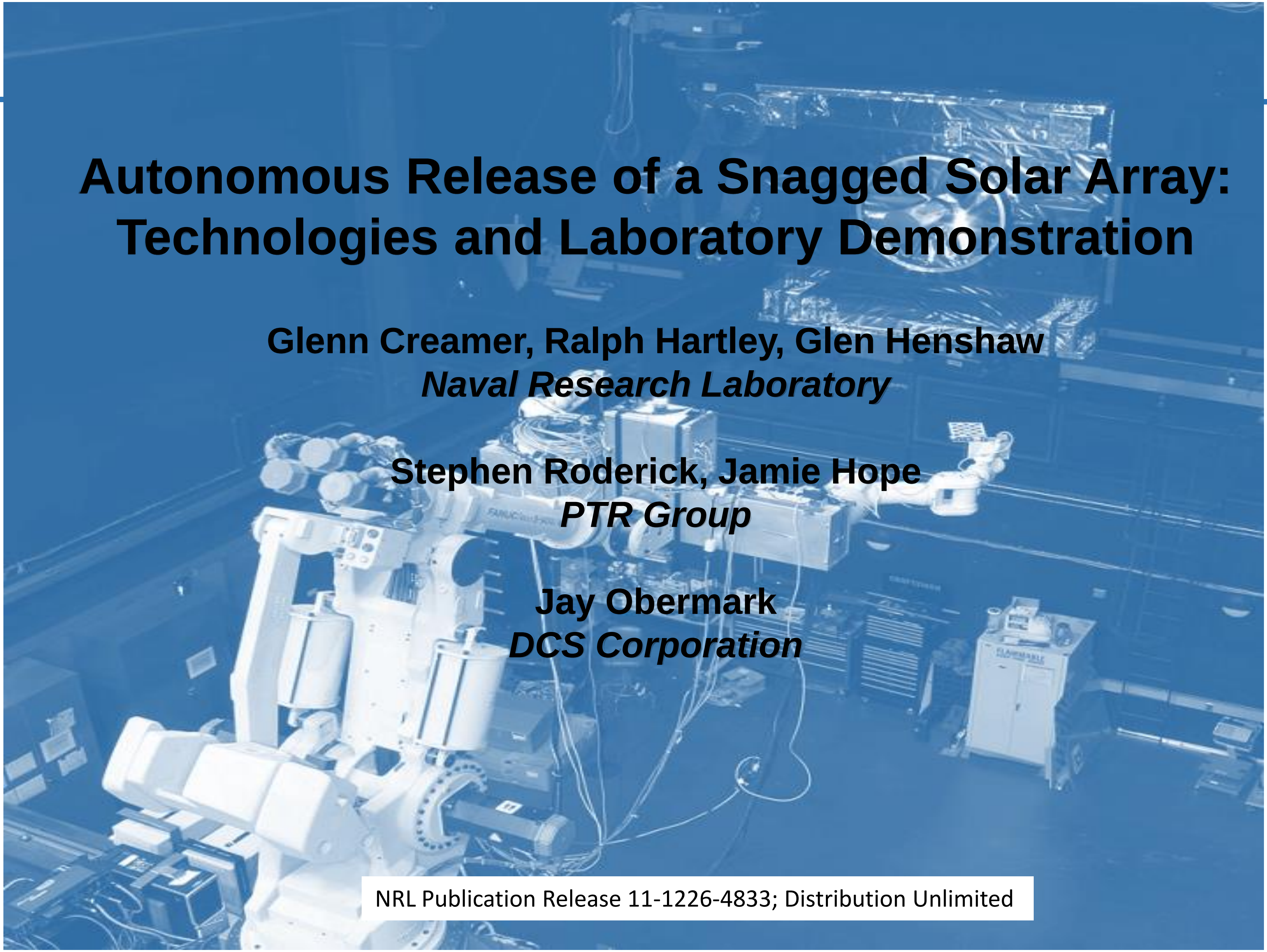

Autonomous Release of a Snagged Solar Array: Technologies and Laboratory Demonstration

Glenn Creamer, Ralph Hartley, Glen Henshaw
Naval Research Laboratory

Stephen Roderick, Jamie Hope
PTR Group

Jay Obermark
DCS Corporation

NRL Publication Release 11-1226-4833; Distribution Unlimited

The Problem

- Solar arrays and antennas can sometimes fail to deploy, resulting in $100s of millions in insurance costs and significant reduction in performance
- While historically rare in occurrence, during 1996-2006 9% of solar array failures were due to deployment malfunctions
- Although the cause of these failures is unknown, it is often possible that a small force would be sufficient to effect a release
- Ground operators attempt to mitigate deployment failures by “shaking” or spinning the satellite, or rotating the satellite in and out of local sunlight…these operations may or may not work

A Solution: Geosynchronous Robotic Servicer

- The most commonly proposed concept for satellite servicing is placement of a general robotic servicer in the geosynchronous belt

- The servicer loiters around the belt until called upon to service a satellite

- The servicer rendezvous with and images the satellite and, upon ground decision and command, approaches the satellite to perform the servicing task

- The servicer would likely require two robot arms, a variety of end effector tools, relative navigation sensors, local imaging sensors, and illuminators.

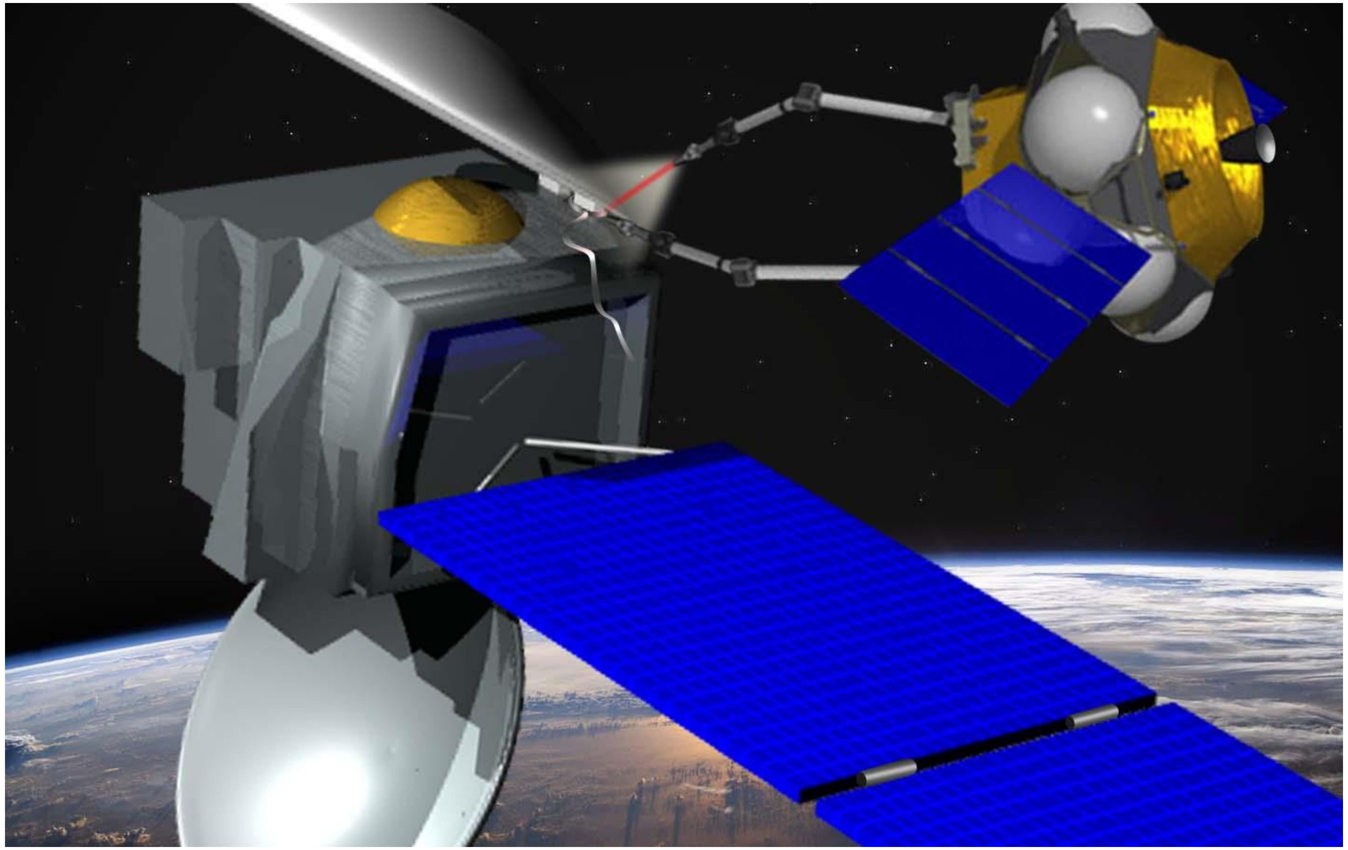

Pre-launch and post-launch calibration routines required to accurately rendezvous and service satellite from servicing arm

Laboratory Robotic Servicer

TriDAR Pose Sensor

Servicing Arm Hardware

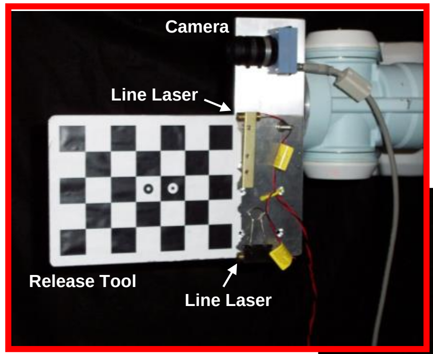

Imaging Arm Hardware

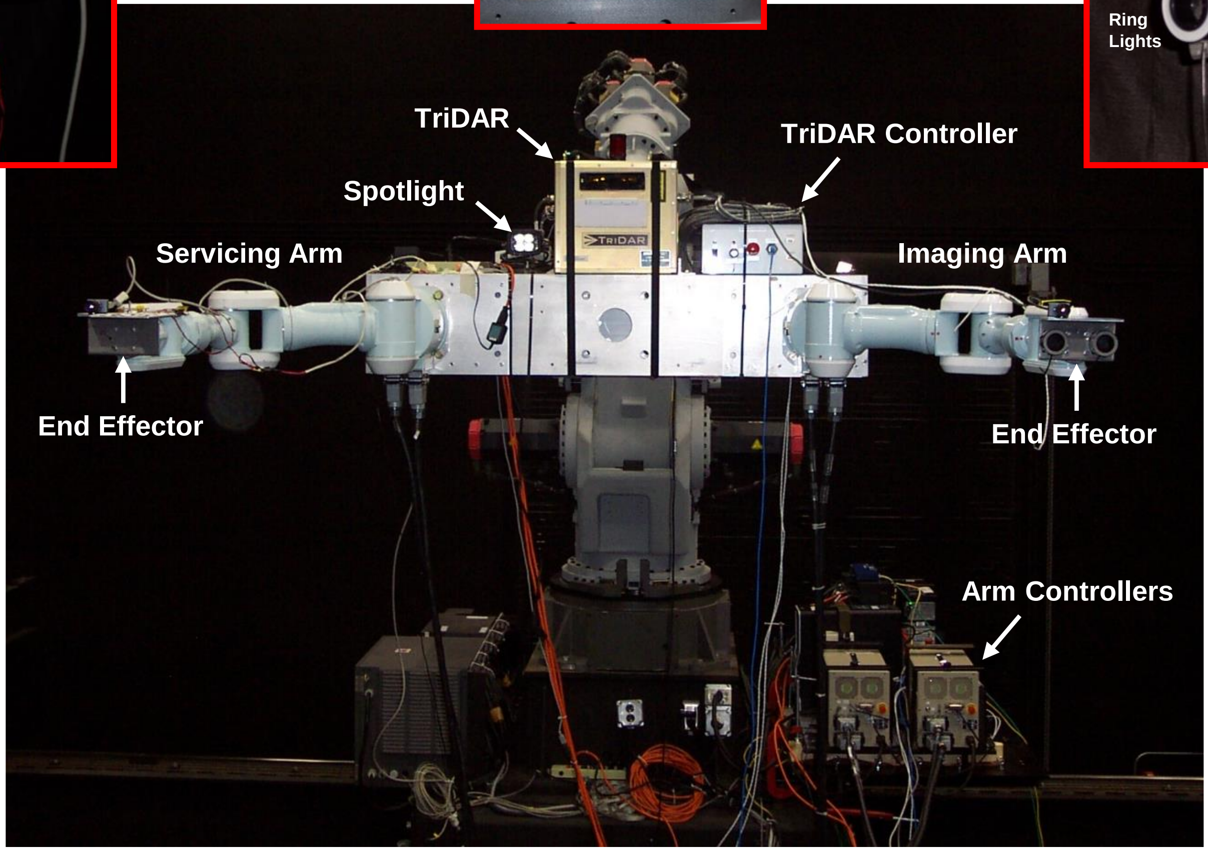

Typical Pose Estimation Results

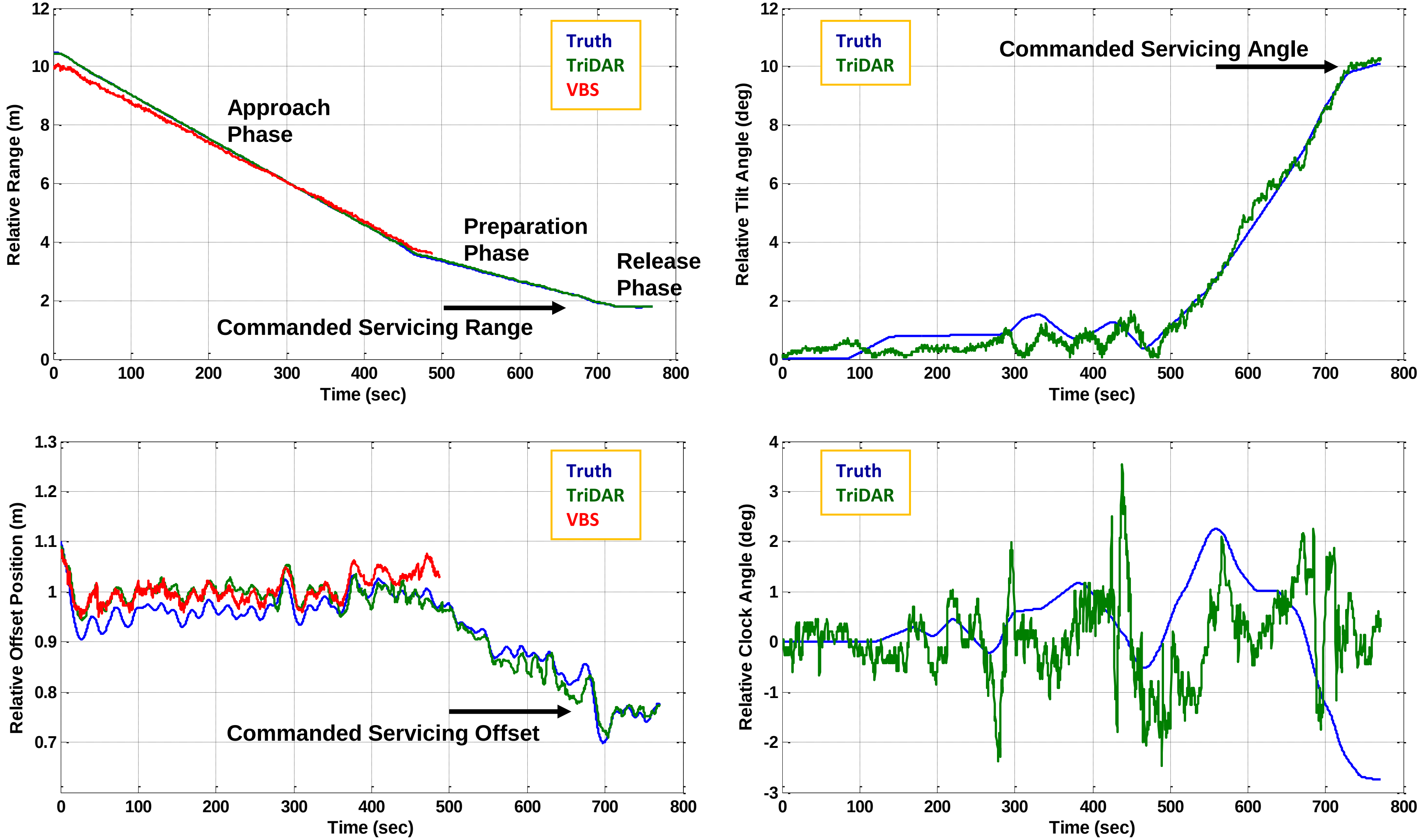

Image from Video of Typical Servicing Test

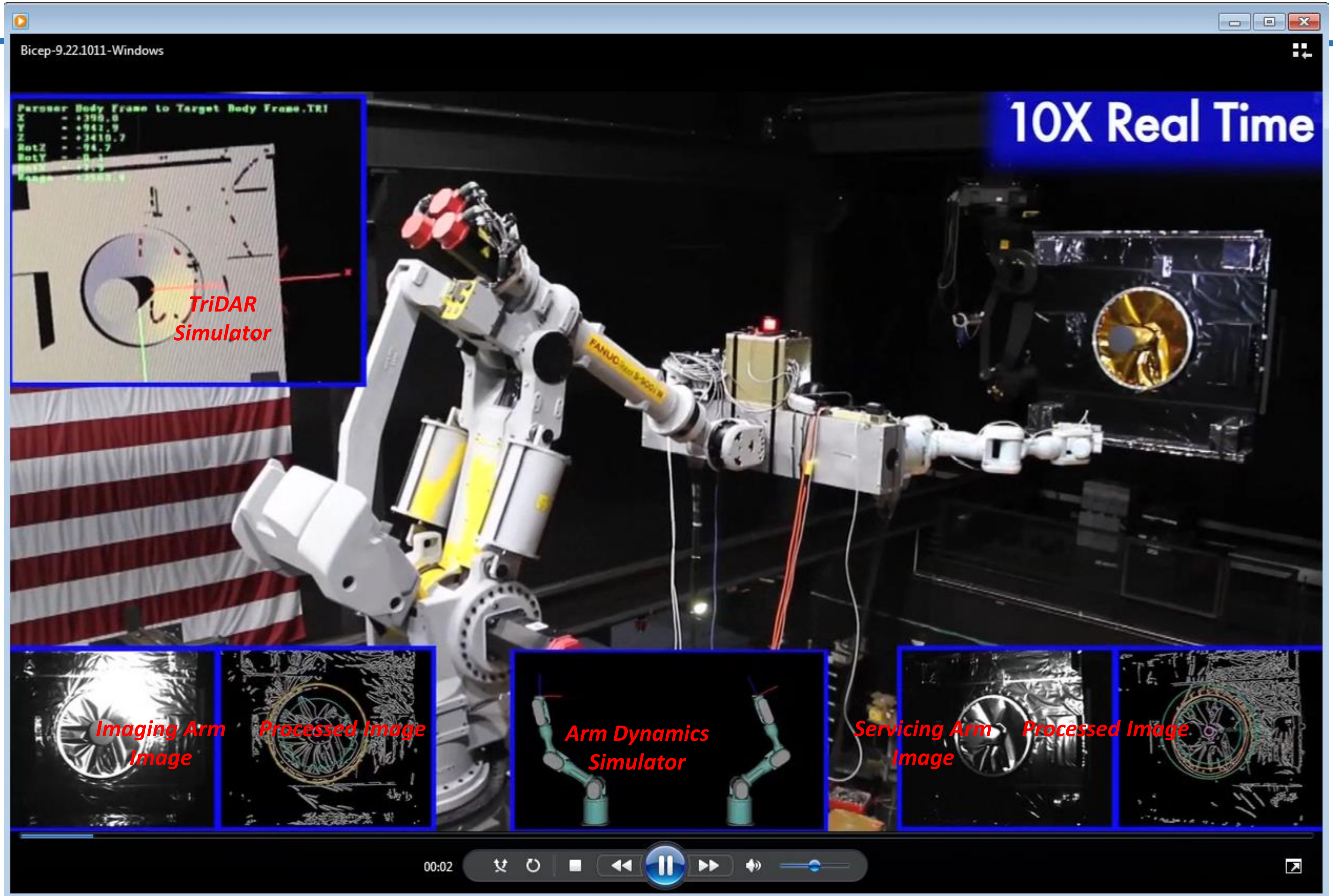

Contact: N. Glenn Creamer, Ph.D., Control Systems Branch, Code 8231, Naval Research Lab., 4555 Overlook Ave SW, Washington, DC 20375; 202-767-0380 Glenn Creamer glenn.creamer@nrl.navy.mil

Mars Hand Lens Imager (MAHLI)

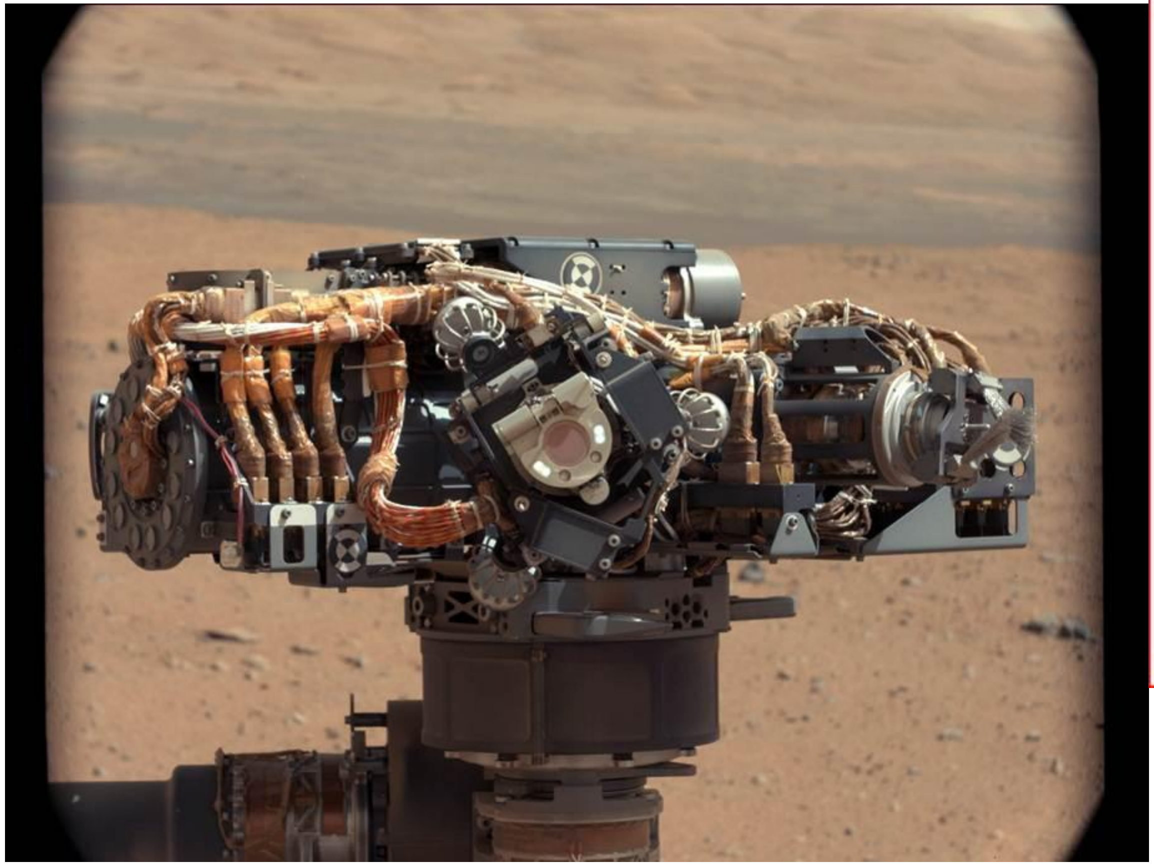

"PIA16161-Mars Curiosity Rover-MAHLI" by NASA/JPL-Caltech/MSSS

Parameter	Value/Description	
Focus	Adjustable; working distances 20.4 mm to ∞	
Focus group range of motion	11.44 mm	
Bandpass	380–680 nm	
Pixel scale	Variable from 13.9 µm/pixel to >>> 13.9 µm/pixel	
Focus-Position Dependent Parameters	25 mm working distance, 15 µm/pixel	∞ working distance
Depth of field	1.6 mm	> 4800 mm
Field of view	34.0° diagonal	39.4° diagonal
Focal ratio	f/9.8	f/8.5
Effective focal length	18.3 mm	21.3 mm
Back focal length	19.8 mm	8.4 mm

Preflight Characterization and Calibration
Cal Tests included characterization of absolute and relative radiometry (required accuracy: 10% absolute, 5% relative), light transfer and noise (e.g., dark current), geometry (focal length, field of view, distortion), resolution (modulation transfer function, point spread function), scattered and stray light, system spectral throughput, and accuracy and precision of the z-stacking range map. Additional tests conducted in after the camera was mounted on the rover, determined the MAHLI boresight, located any onboard noise sources, and characterized the robotic arm's MAHLI positioning capabilities and verify contact sensor performance.
Calibration on Mars
MSL carries the MAHLI Flight Calibration Target for color/white balance, resolution and focus checks, and verification of UV LED functionality.

2014 CALCON

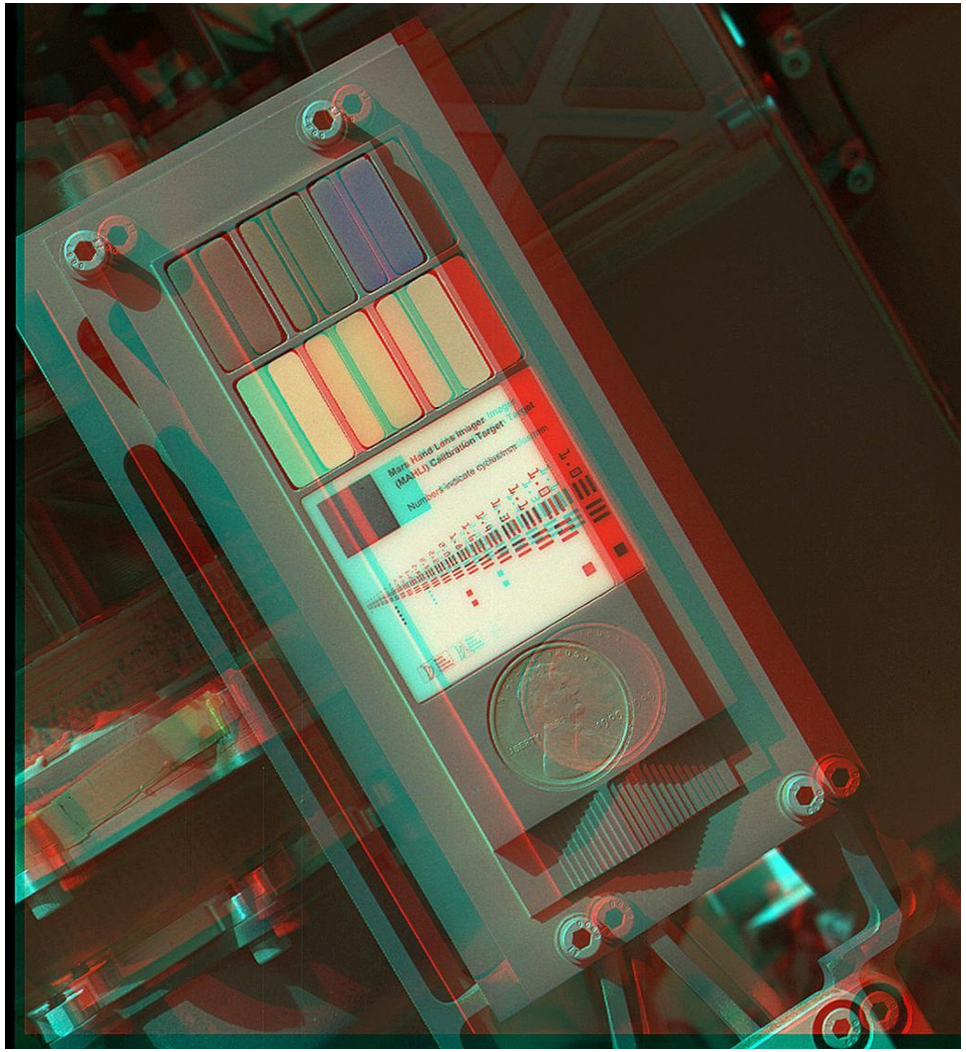


Mars Hand Lens Imager
(MAHLI) Calibration Target
Numbers indicate cycles/mm

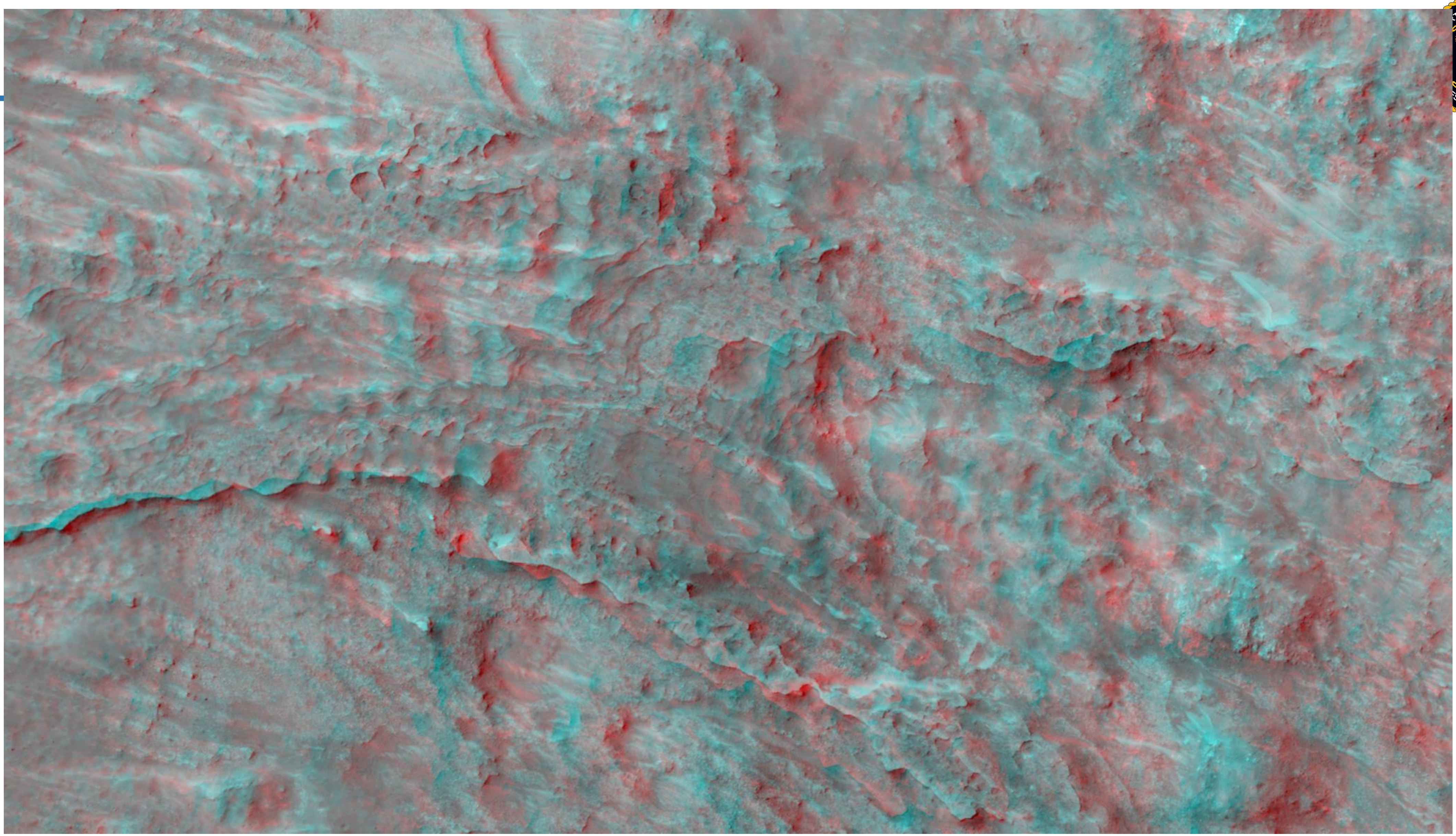

Hi-RISE, NASA/JPL-Caltech/University of Arizona

This image show layers and fans on the floor of a large ancient impact crater. The shape of the fans indicate that water was involved in their formation http://stereo.gsfc.nasa.gov/img/3dimages/movies/3D_EUV195_0507.mpg

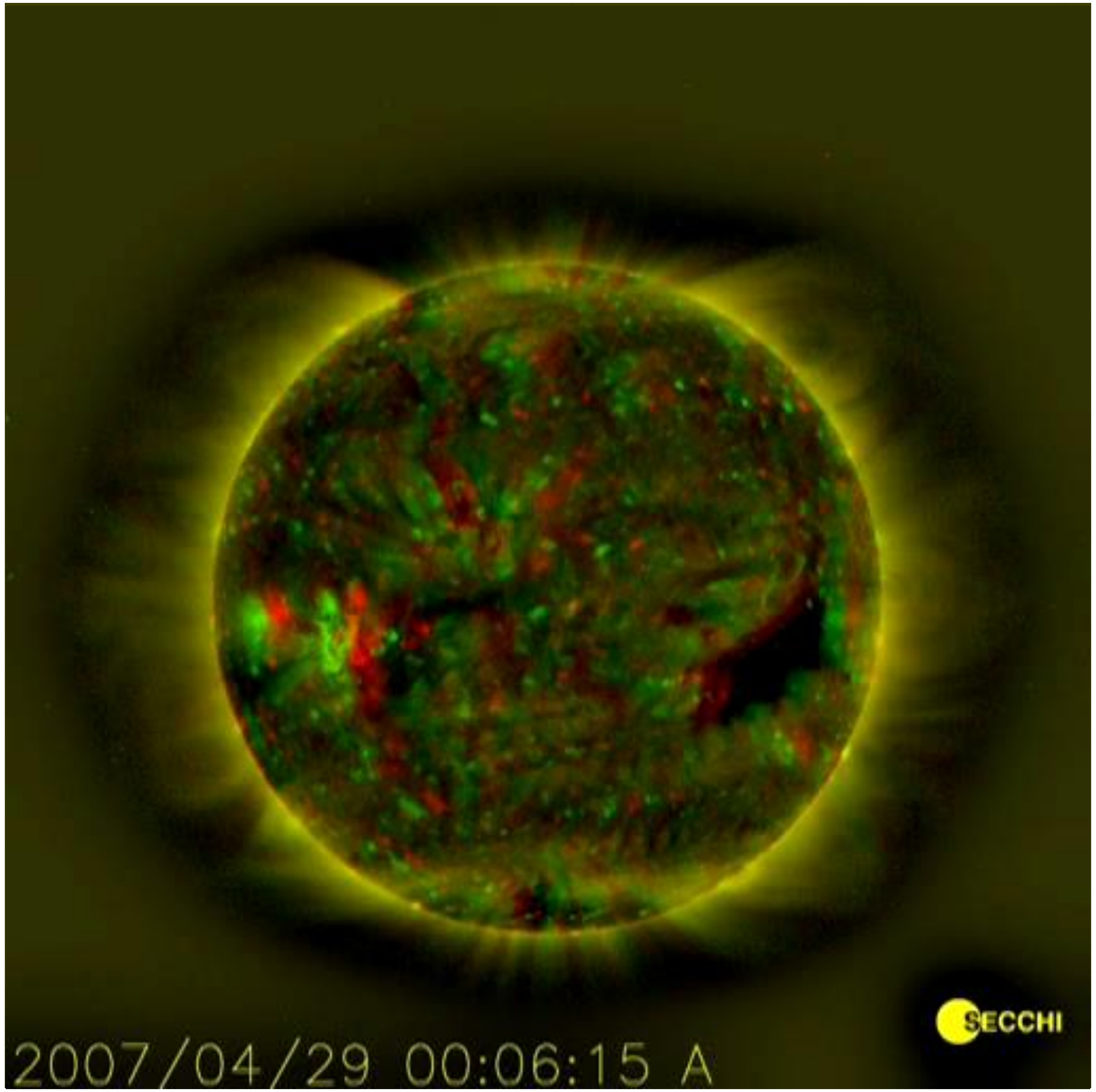

About the STEREO Mission

STEREO (Solar TErrestrial RElations Observatory) is the third mission in NASA's Solar Terrestrial Probes program (STP). It employs two nearly identical space-based observatories - one ahead of Earth in its orbit, the other trailing behind - to provide the first-ever stereoscopic measurements to study the Sun and the nature of its coronal mass ejections, or CMEs.

STEREO'S SCIENTIFIC OBJECTIVES ARE TO:

- Understand the causes and mechanisms of coronal mass ejection (CME) initiation.
- Characterize the propagation of CMEs through the heliosphere.
- Discover the mechanisms and sites of energetic particle acceleration in the low corona and the interplanetary medium.
- Improve the determination of the structure of the ambient solar wind.

http://stereo.gsfc.nasa.gov/links.shtml

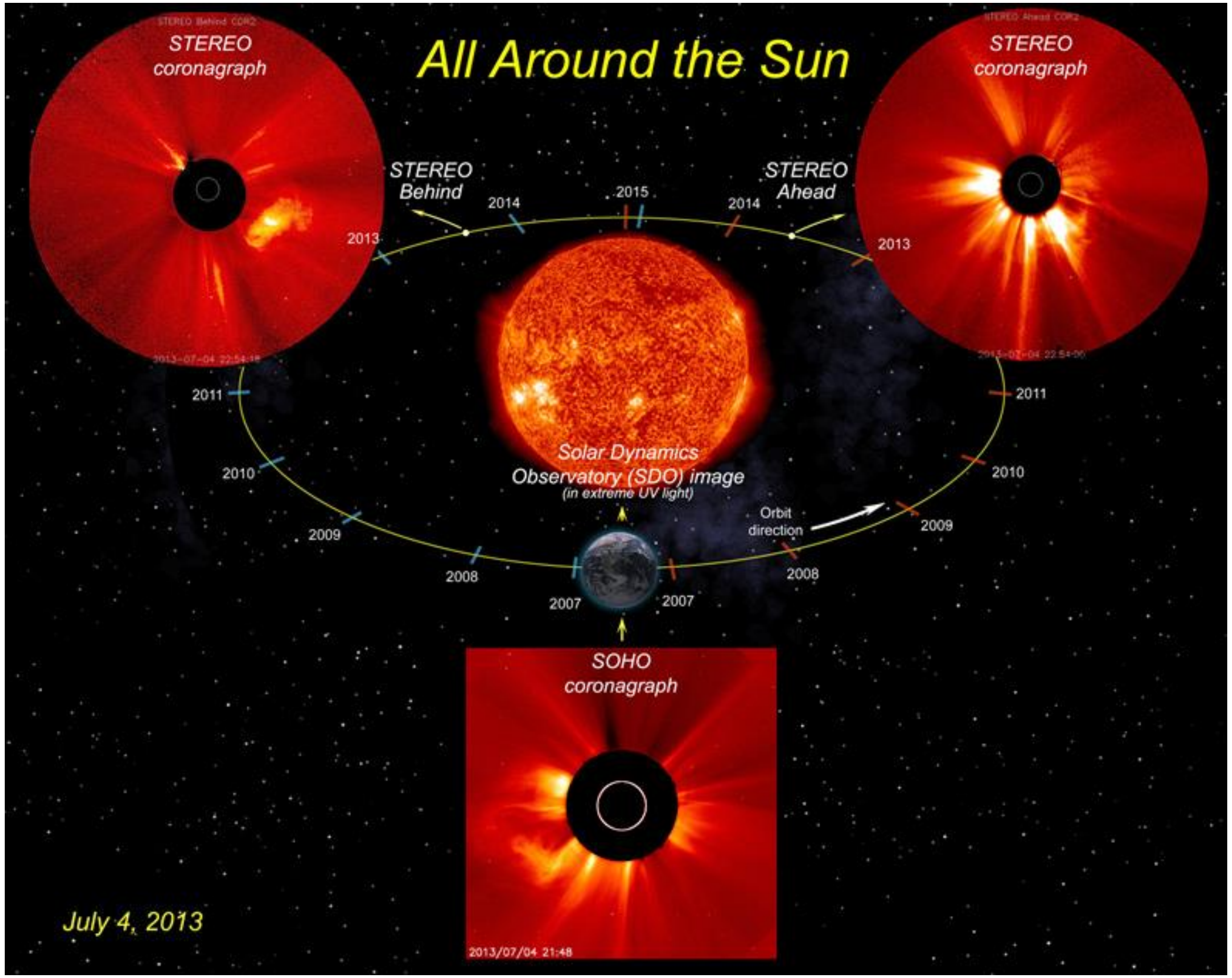

Oh By the Way…

A CME erupted and zoomed toward earth at 3000 km/s - Almost 4 times faster than average CME bursts.

The CME's trajectory was earth's orbit. Fortunately, the earth was not there. Instead, the CME hit STEREO A.

Damage such an event could have is estimated
To be in the billions due to the interconnectedness of our power grids.

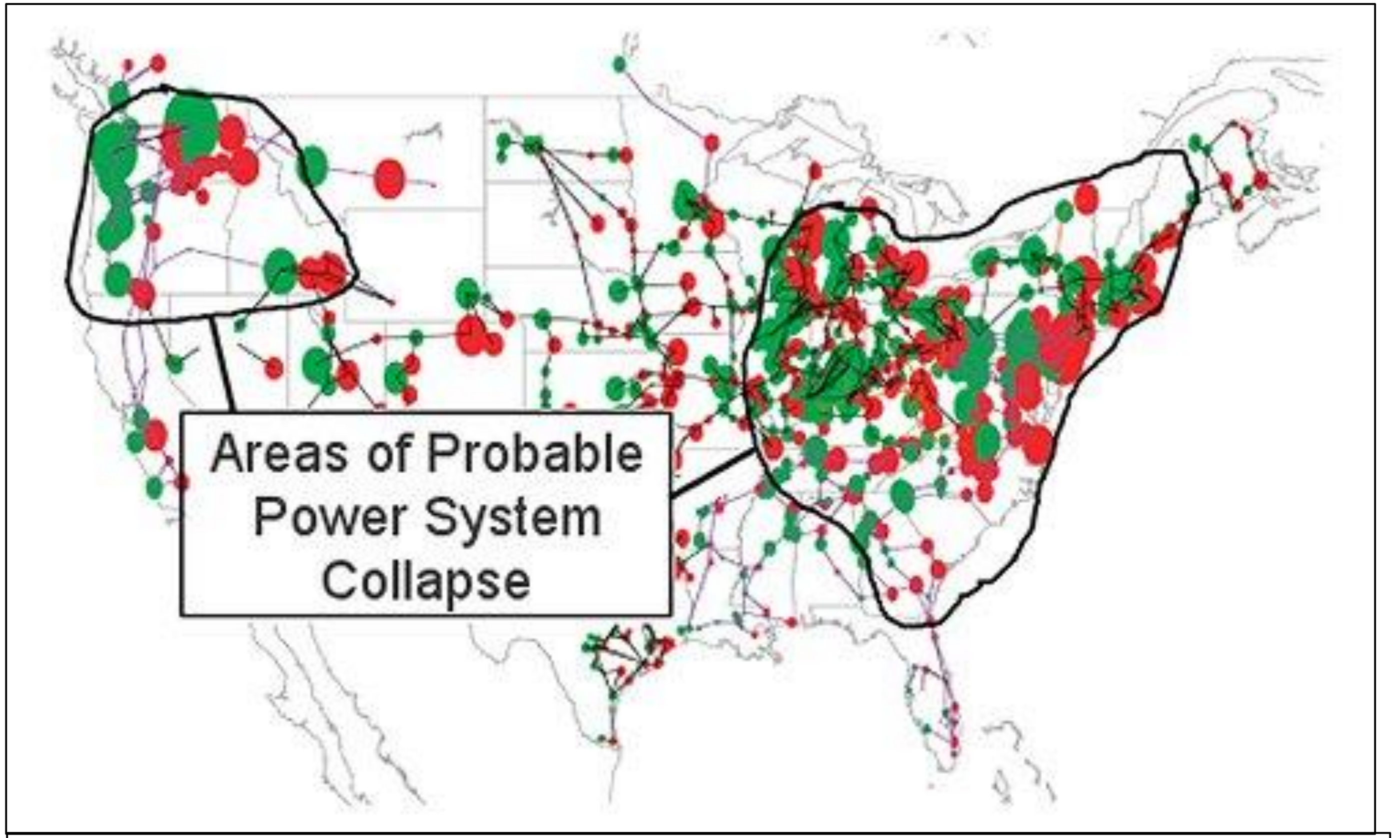

Figure from "Severe Space Weather Events: Understanding Societal and Economic Impacts", National Academy of Sciences, 2008

Ultimate Calibration Challenge

Search for the Higgs Boson….

Establish a Reference from which to detect evidence of the Higgs Boson.

Very very complex effect with very very big instrument!

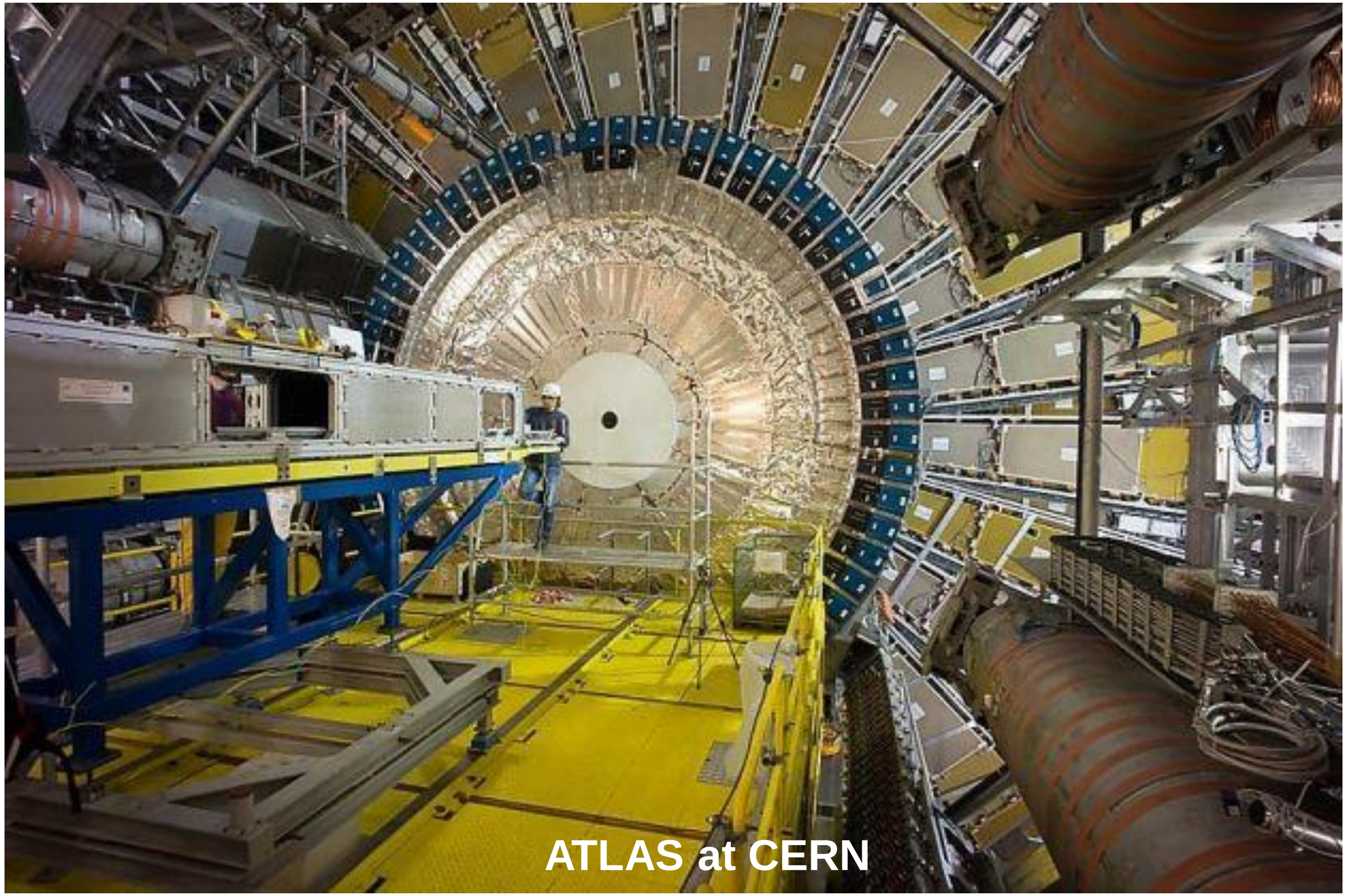

If the particle's mass is about 115GeV, then "The Standard Model" Prevails

If the particle's mass measures abut 140 GeV, then a Multi-Verse Model holds

CERN measured the Higgs Boson to have a mass of 125 GeV.

Almost in the middle !!

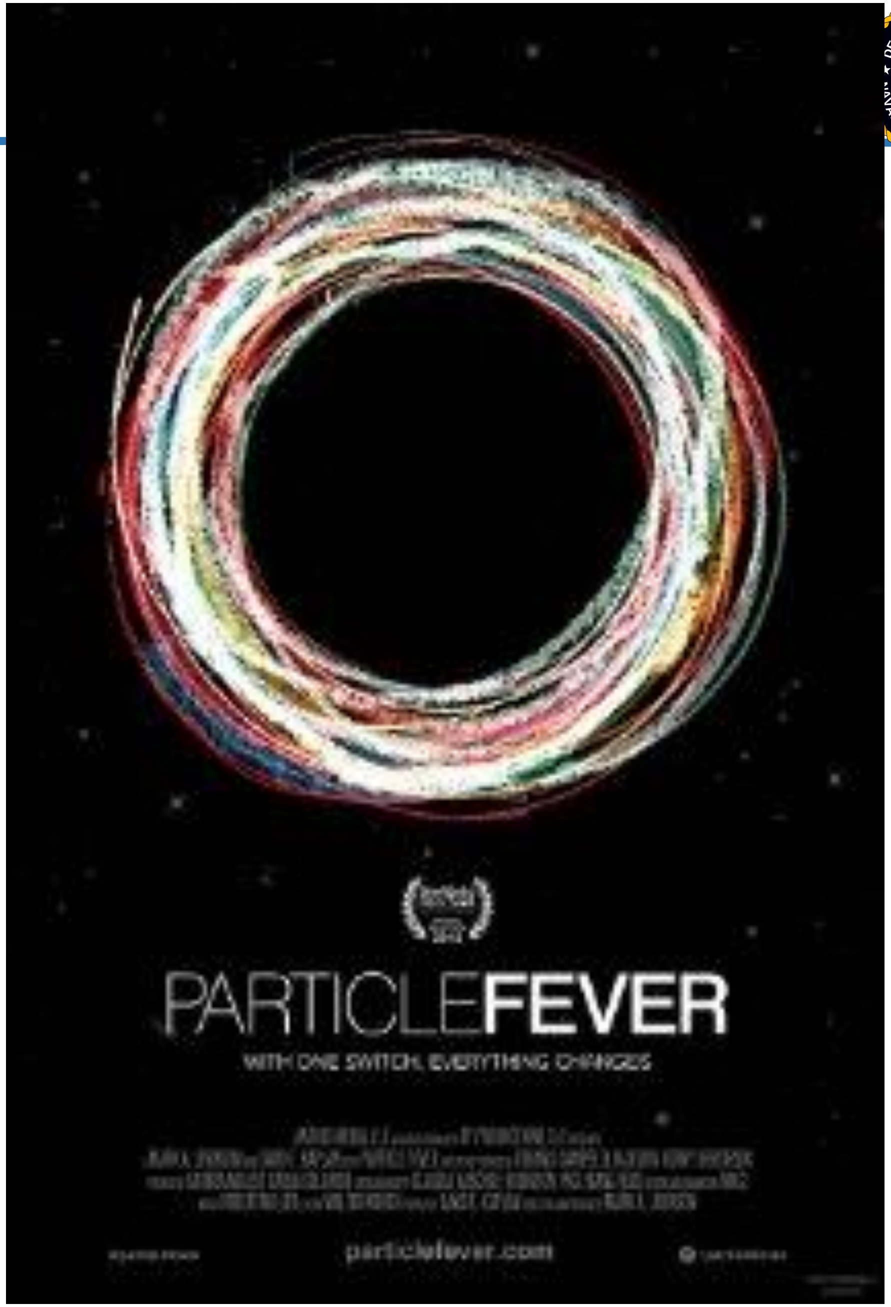

Link to Video

Challenges & Creativity

- Problem Solving is inherently creative
- In calibration for remote sensing, machine vision, mass spectroscopy, etc, the challenges lay between:
    - Theory and Experiment.
    - Software and Hardware

Example: Detection of Small signals in close proximity to systematic signals:

- If we filter out the signals with hardware (bandpass filters), we increase signal-to-noise by reducing noise and clutter but potentially miss important information.
- If we open up the bandpass, we swamp our circuits, memory, and sensor capability.

How we balance software/algorithms with hardware is the ART of signal science and the creative soul of calibration. Essentially, is it noise or not?

If you have a good idea…


Never Give Up – Never Surrender
Galaxy Quest

Extras

Servicing Mission Concept of Operations

Initial Rendezvous

Rendezvous with the target satellite is achieved using both ground-based orbit knowledge and relative navigation sensors such as Vis/IR cameras and TriDAR

Navigation Source	Rendezvous Range
Ground-Based	10 km
Vis/IR Imaging	1 km
Vis/IR/TriDAR	50 m

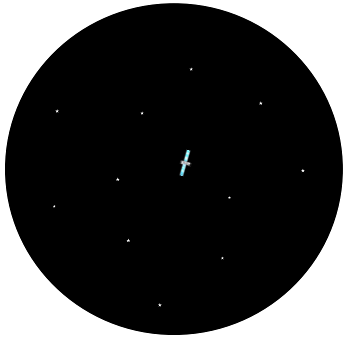

Close Proximity Imaging

The servicer approaches the target using TriDAR, generates visible and 3D images of the area of interest, then backs off to a safe-hold station

Visible image of satellite back face

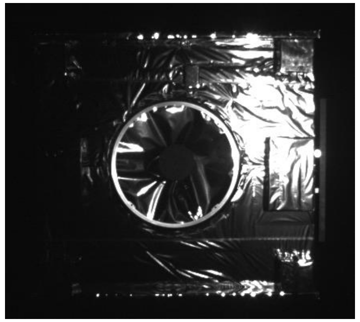

3D image of satellite back face

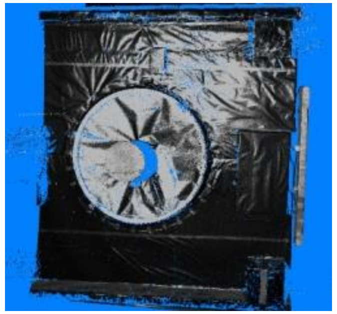

Ground Planning

Images are analyzed to determine the best servicing strategy to release of the stuck deployable, as well as the preferred approach path and station-keeping box the servicer needs to track

Autonomous Servicing

The servicer autonomously follows the commanded approach path, positions itself within the station-keeping box, and performs release of the array

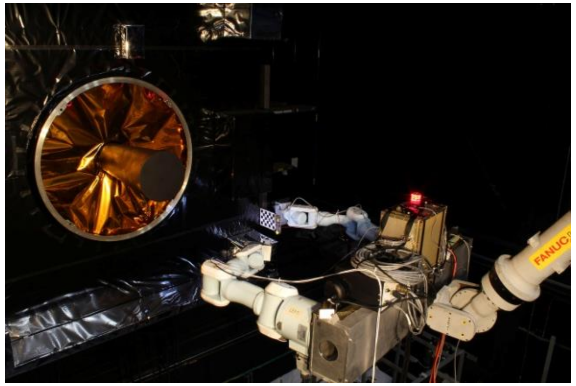

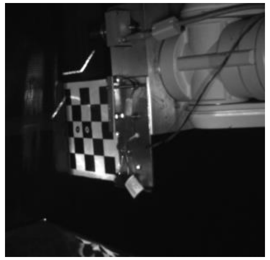

Tool Insertion in Gap

Calibration of the MX-20SW Standoff SWIR Hyperspectral Imaging Ball Gimbal System

Jonathan G. Neumann, Eric C. Allman, Trijntje V. Downes, J. Grant Howard, Mel K. Kruer, John N. Lee, Dale Linne von Berg, Robert A. Leathers, Jeremy Murray-Krezan, Nicholas Nezis
Naval Research Laboratory
Michael Colbert, Steve Frawley
Smart Logic, Inc.

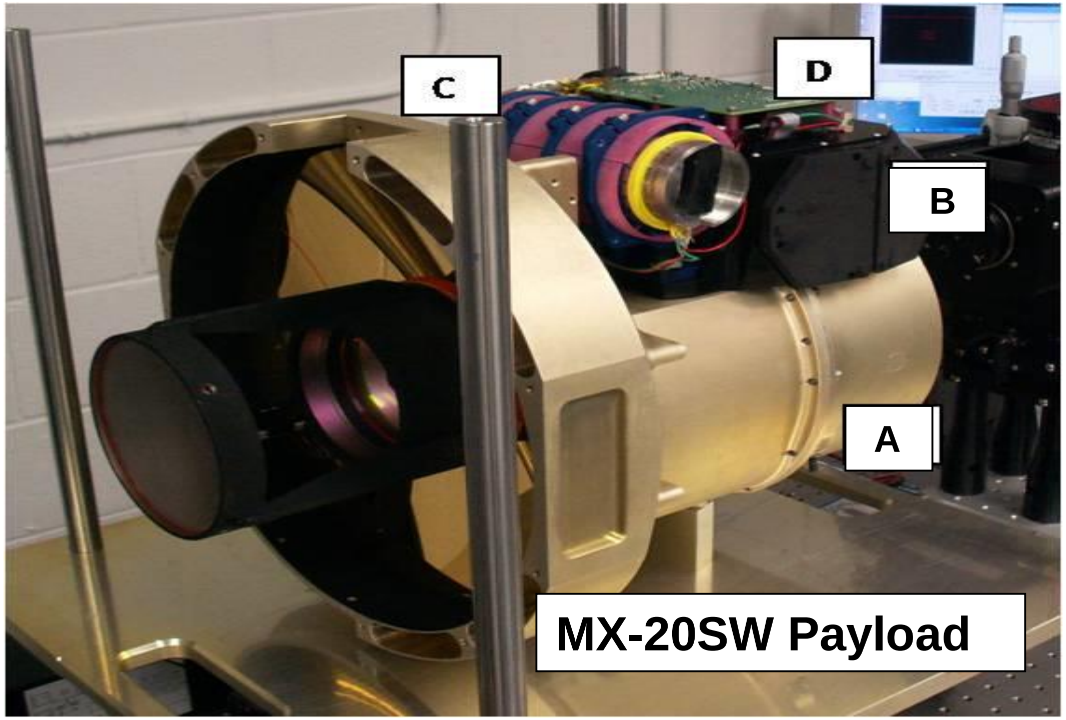

(A) Foreoptics / Optical Housing: L-3 Applied Physics Specialties, L-3 Wescam
(B) Spectrometer: Brandywine Optics, Inc, Welch Mechanical Designs, LLC
(C) Detector / Dewar / Compressor: Raytheon Vision Systems
(D) Read-out Electronics: Smart Logic, Inc.

NRL Publication Release No.: 8-1221-1741; Distribution Unlimited

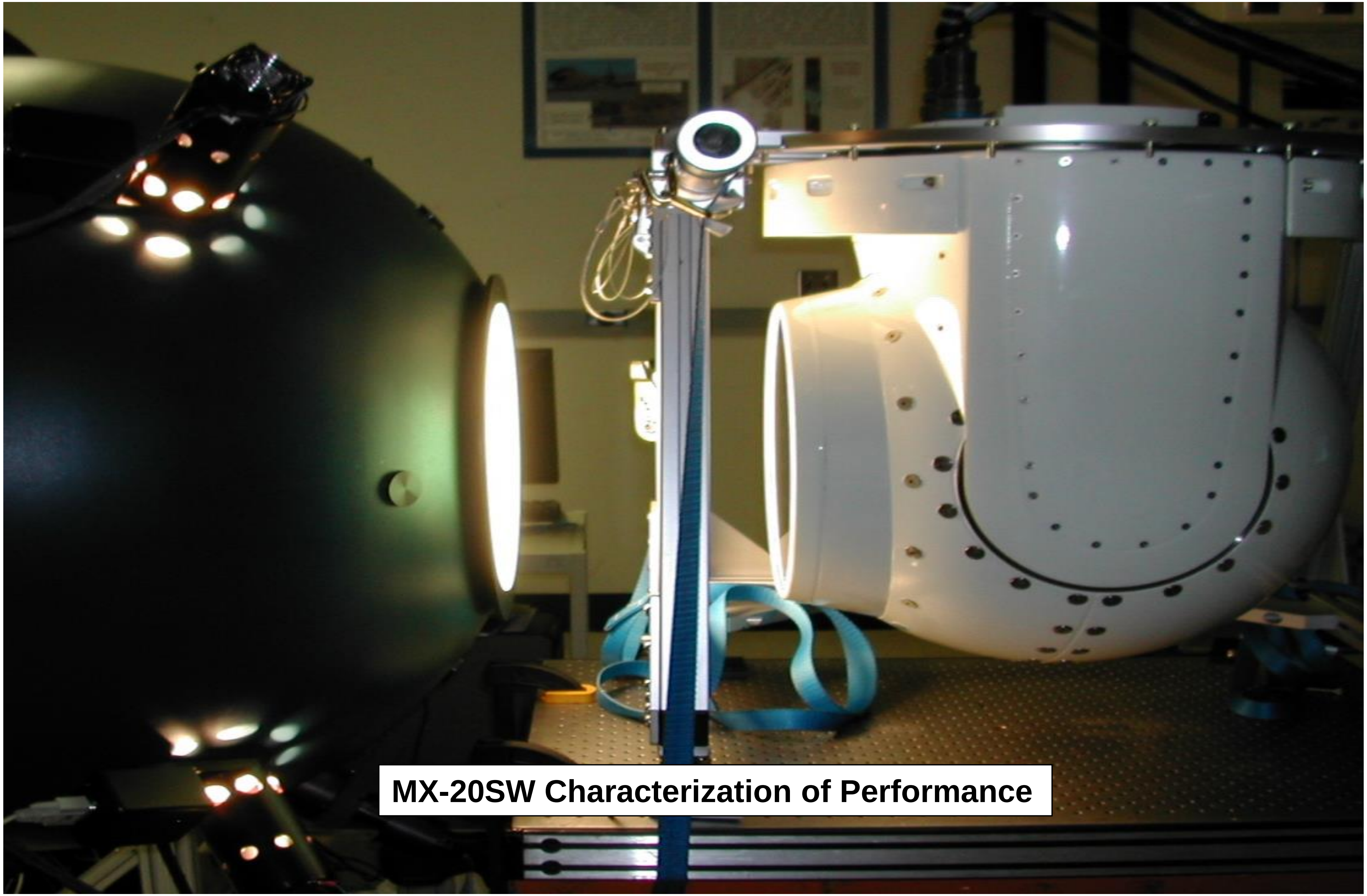
MX-20SW Characterization of Performance

MX-20SW Spectral Calibration

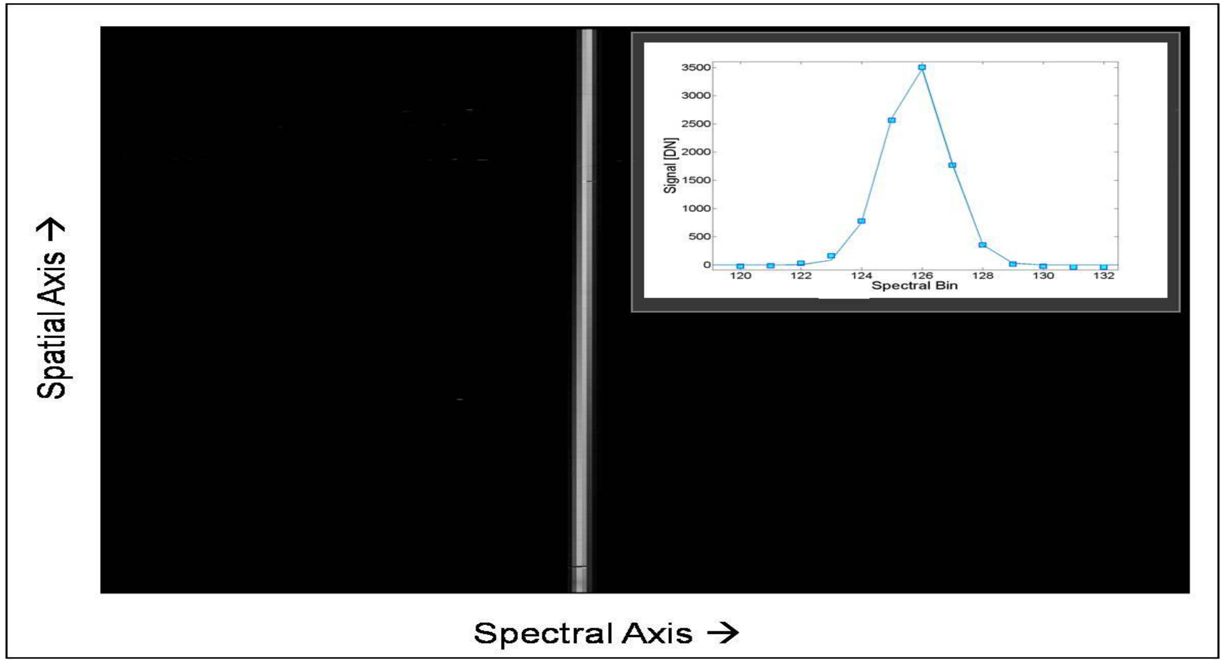

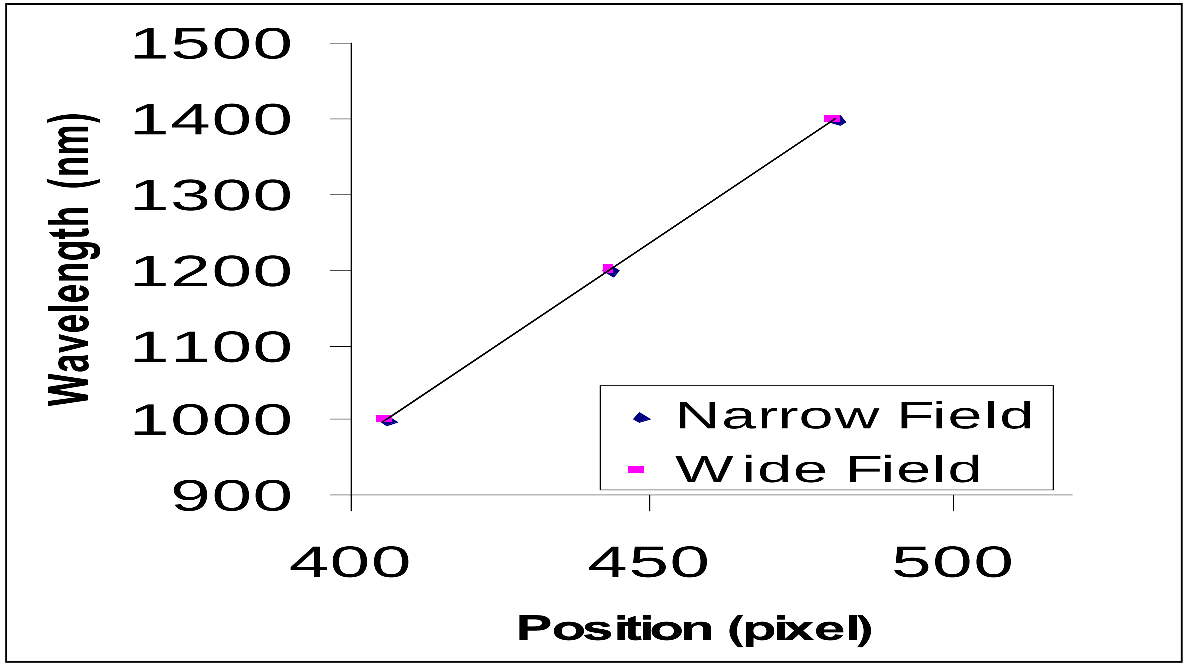

Image of FPA:
Source = Labsphere viewed through 1200 nm Filter

Wavelength = 5.34 (position) – 1183.7

MX-20SW Characterization – Noise / Sensitivity

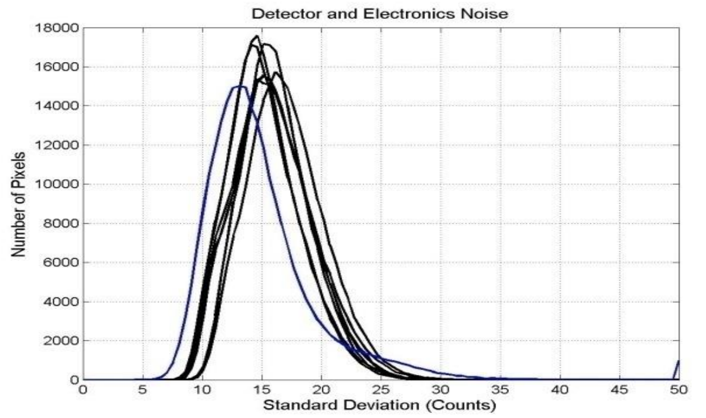

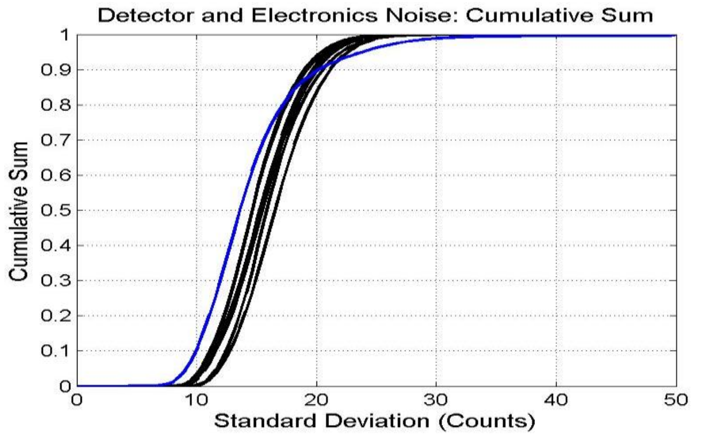

Shutter Employed for Dark Frames
Noise μ/σ = 16.4 / 3.2 counts
Read-out = 8.9 counts

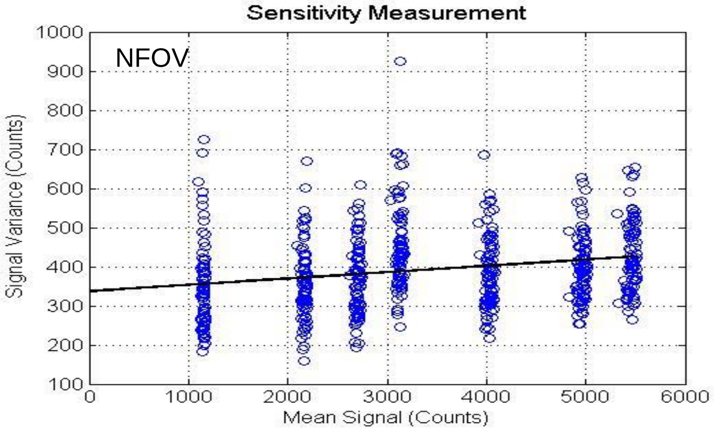

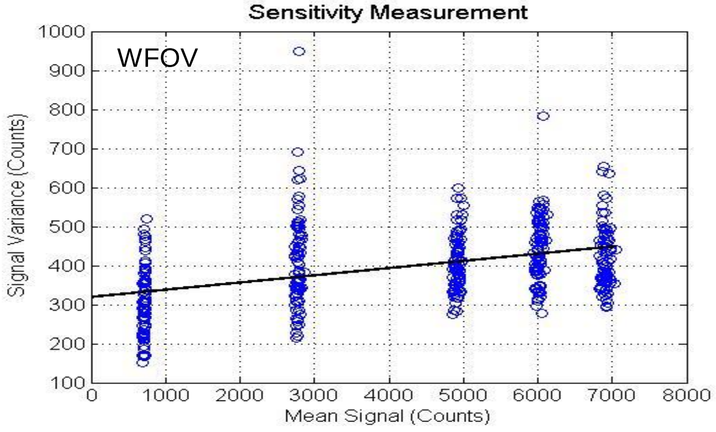

Wide Field of View:
Mean Responsivity = 1.04 μflicks
Sensitivity = 17.5 μflicks

Narrow Field of View:
Mean Responsivity = 2.5 μflicks
Sensitivity = 41.6 μflicks

Data from all “good” pixels in array

$$\text{Responsivity}(\lambda) = \frac{hc(e_{DN})}{\lambda\, t_o \eta(\lambda) \tau \Delta\lambda\, A_o (IFOV)^2}$$

N. Kopeika, "A System Engineering Approach to Imaging". SPIE Press, 1998.